Analysis of Heat Transfer and Flow over a Backward Facing Step

A Dissertation submitted
in partial fulfilment of the requirements
for the award of degree of

Master of Engineering

in

Thermal Engineering

by

Umesh

Registration No.: 801483024

Under the Supervision of

Mr. Kundan Lal
(Assistant Professor)

Dr. Dwarikanath Ratha
(Associate Professor)

DEPARTMENT OF MECHANICAL ENGINEERING

THAPAR UNIVERSITY, PATIALA

July, 2016

CERTIFICATE

I hereby declare that the thesis entitled "**An Investigation of Heat Transfer and Flow over a Backward Facing Step** " is an authentic record of my work carried out as requirements for the award of the degree of **Master of Engineering** in **Thermal Engineering** at **Thapar University, Patiala** under the supervision of **Mr. Kundan Lal**, Assistant Professor, Mechanical Department, Thapar University, Patiala and **Dr. Dwarikanath Ratha**, Associate Professor, Civil Department, Thapar University, Patiala during July, 2014 to July, 2016. No part of the matter embodied in this report has been submitted to any other university or institute for the award of any degree.

Umesh

Date: 13-07-2016

Umesh

It is certified that the above statement made by the student is correct to the best of my/our knowledge and belief.

Mr. Kundan Lal
Assistant Professor, MED
Thapar University, Patiala

15/7/16

Dr. Dwarikanath Ratha
Associate Professor, CED
Thapar University, Patiala

Countersigned by

Dr. S.K. Mohapatra
Head, Mechanical Engineering Department
Thapar University, Patiala-147004

Dr. S.S. Bhatia
Dean of Academic Affairs
Thapar University, Patiala-147004

Dedication

I dedicate this thesis to my beloved father Satyaprakash Sharma and my mother Krishna Devi, who are an ever supporting and encouraging with their great patience. I also dedicate this to all my dearest friends.

Acknowledgements

First of all, I would like to thanks to my most esteemed supervisors Dr. Dwarikanath Ratha and Mr. Kundan Lal for their worthy guidance, continuous encouragement and having high patience to listen to all my queries and suggest accordingly. The faith of Dr. Dwarikanath Ratha and Mr. Kundan Lal in me always compelled me to work hard, apart from thesis their attitude towards life, work and valuable words taught me many things.

I appreciate the facilities provided by Thapar University to carry out my studies and gain practical knowledge.

A special debt of gratitude is owed to the authors whose work I have consulted and quoted in this work.

Last but not least I am always grateful to my family and friends for their unconditional support, encouragement and best wishes, without which I have not come this far.

Umesh

Umesh

Abstract

Flow over a backward facing step along with heat transfer is studied for two and three dimensional vertical as well as curved backward facing step using ANSYS Fluent. The mesh is generated using ICEM software in ANSYS. The grid independency test is performed to make the results independent of the grid size after a particular number of elements. The reattachment length and Nusselt number are calculated for a wide range of Reynolds number covering both laminar and turbulent flow. The results obtained in the present study have been validated with published literature. Also the reattachment length and Nusselt number are calculated for various expansion ratios. The reattachment length is observed to decrease with increase in the expansion ratio for laminar flow whereas reattachment length is found to be increasing with increase in the expansion ratio for turbulent flow when expansion ratio is varied by changing the inlet channel height. The reattachment length is found to be increasing with expansion ratio for all laminar, transition and turbulent regimes when expansion ratio is varied by changing the step height. The reattachment length is also found to be less for curved backward facing step as compared to the vertical backward facing step.

The results for the Nusselt number are calculated for wide range of Reynolds number incorporating both the laminar and turbulent flow. The value of Nusselt number is observed to increase with the Reynolds number both in laminar and turbulent case. The steep increase in the Nusselt number is found as we stepped into the turbulent flow at Reynolds number 2500. The results for Nusselt number are also compared for vertical backward facing step and curved backward facing step. The peak of the Nusselt number is observed to be shifted towards left for the curved backward facing step as compared to the vertical backward facing step due to decrease in the reattachment length for the curved backward facing step.

The various flow characteristics are also obtained for vertical as well as for the curved backward facing step for laminar as well as turbulent flow. The results obtained from the curved backward facing step are compared with the vertical backward facing step.

Keywords: Backward facing step; Reattachment length; Heat transfer; Laminar flow; Turbulent flow.

Table of Contents

List of Figures

List of Tables

List of Symbols and Abbreviations

Nomenclature

h	:	Height of inlet channel
H	:	Height of channel downstream of the step
S	:	Step height
L	:	Spanwise width
Xe	:	Length of the channel upstream of step
Xo	:	Length of channel downstream the step
d	:	Hydraulic diameter
u, v, w:		Component of velocity in x, y and z direction respectively
Re	:	Reynolds number
k	:	Turbulence kinetic energy
Nu	:	Nusselt number
Xr	:	Reattachment length

Greek symbols

μ	:	Dynamic viscosity of fluid
ρ	:	Fluid density
C_p	:	Specific heat
K	:	Thermal conductivity of fluid

Acronym

BFS	:	Backward Facing Step
PIV	:	Particle Image Velocimetry
ER	:	Expansion Ratio
AR	:	Aspect Ratio

Chapter 1

Introduction

1.1 Introduction

The flow structures formed during the flow over backward facing step includes two most frequent phenomenon separation and reattachment. Such kind of flow pattern influences the heat transfer characteristics of the flow which is of great importance in many heating and cooling applications like heat exchangers, gas turbine engines, electronic cooling equipments, combustors and in many other heat transfer devices. The application of this geometry lies not only where this shape is used but also where there is separation and reattachment regions develop like flow over aerofoil, flow around building and many external flows. The reason being chosen this geometry attributes to its simplicity to analyse the complex behaviour of the flow which makes the backward facing step as the key choice for many authors to conduct the study of flow and heat transfer both experimentally and numerically. Armaly et al. [1983] conducted the experimental and theoretical study of flow over the two dimensional backward facing step. They obtained the results for Reynolds number range covering the laminar, transition and turbulent flow against the reattachment length. The results show that the reattachment length increases in the beginning with Reynolds number and later decreases and vanishes above a Reynolds number of approximately Re>6600. Kondoh et al. [1993] carried out the computational study for laminar heat transfer downstream of a backward facing step for different values of expansion ratio, Reynolds number and Prandtl number. They found that Nusselt number increases with both Re and ER. Iwai et al. [2000] studied the flow and heat transfer characteristics of laminar flow over the backward facing step in a rectangular duct. The results obtained show that the peak Nusselt number did not occur on the centre line but near the side walls. Togun et al. [2014] presented the numerical study of laminar flow and heat transfer over a backward facing step with and without obstacle. The increase in heat transfer coefficient and consequently the rate of heat transfer was noted with the use of obstacle as compared to backward facing step without obstacle. Ratha and Sarkar [2014] investigated the flow past a backward facing step with transition. It was noted that the primary reattachment length is minimum for round edged step and maximum for the vertical step.

The following sections will deal with the geometric specification of the backward facing step. Then basic flow behaviour past a backward facing step followed by need, objective and applications of the current study will be discussed.

1.1.1 Description of geometry of backward facing step

Figure 1.1 shows the geometric parameters of a three dimensional backward facing step. The geometry parameters include the height of the channel upstream and downstream of the step, expansion ratio and aspect ratio.

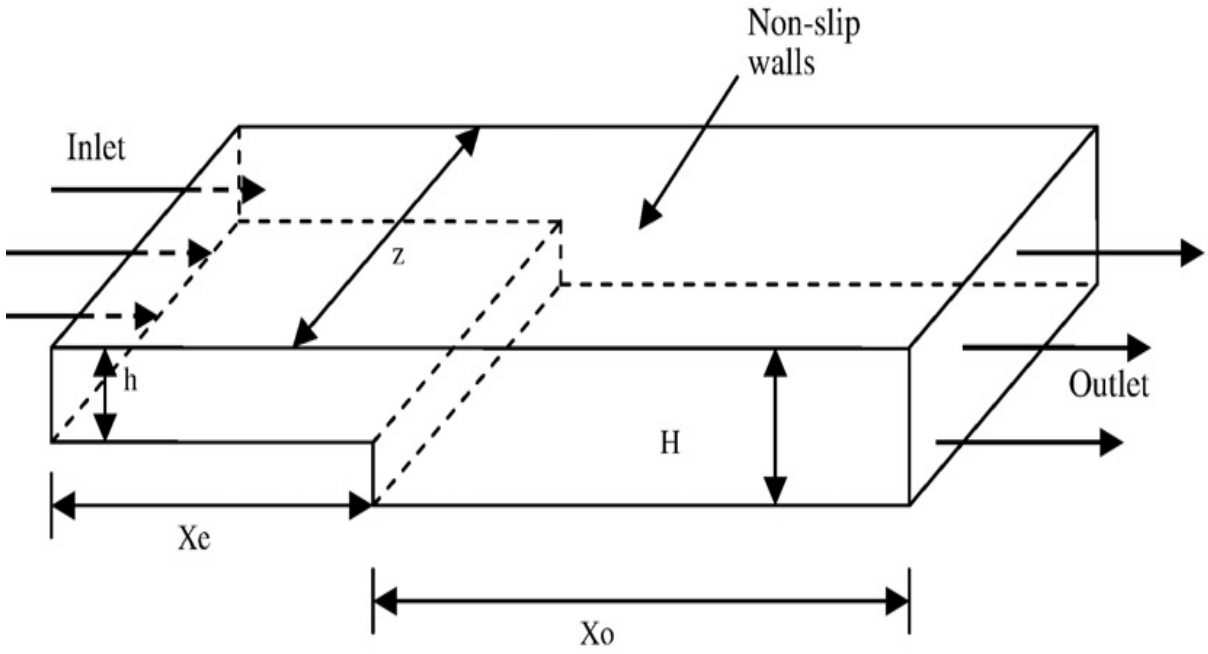

Figure 1.1: Schematic of backward facing step [Lima et al., 2008]

Height of inlet channel	h
Height of sudden expansion	H
Spanwise width	Z
Step height	S
Inlet channel streamwise length	Xe
Outlet channel streamwise length	Xo

Expansion ratio (ER):

The expansion ratio can be defined as the ratio of downstream height to upstream height of the channel at the step location. ER=H/h

Aspect ratio (AR):

The aspect ratio can be defined as the ratio of width to height of backward facing step.

AR=Z/S

1.1.2 Flow over backward facing step

Figure 1.2 shows the flow past a backward-facing step developing recirculation zones where the separation of fluid occurs and vortices are formed. For turbulent flow, the fluid separates at the step and reattaches downstream. Only a single recirculation zone is formed for turbulent flow. Separation occurs when adverse pressure gradients are present in the fluid. As the Reynolds number increases from zero, the first region of separation occurs at the step on the bottom wall where negative velocities are present. Next, the second region of recirculation formed on the upper wall. As the Reynolds number increases further into the transition zone, a third recirculation region is formed on the bottom wall [Armaly et al., 1983].

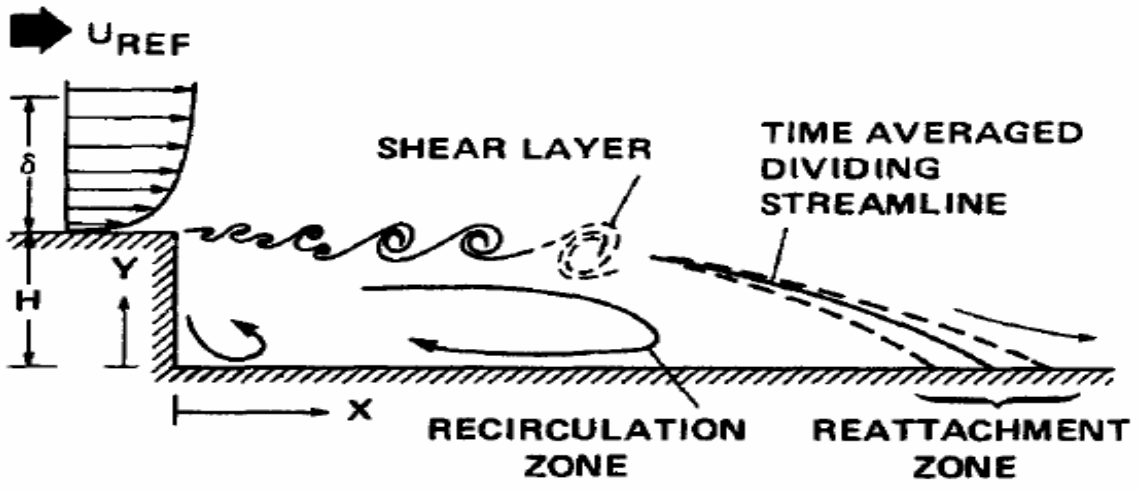

Figure 1.2: Flow over a backward facing step [Source: Simpson, 1996]

1.2 Need of present study

In the literature referred so far it is found that a number of researchers have conducted the study of flow over backward facing step to study the effect of Re and expansion ratio on reattachment length. But a few literatures is available on analysis of heat transfer and even less literature is prevailing for study of turbulent flow and heat transfer over three dimensional backward facing step. And there is almost no literature is available to study the heat transfer for a curved backward facing step. Hence in the current study a numerical study using FLUENT is conducted to analyse the flow and heat transfer for both two dimensional and three dimensional cases including vertical and curved steps.

1.3 Objectives of present study

1. To study the effect of Reynolds number on reattachment length for vertical as well as curved backward facing step.

2. To study the effect of Reynolds number on rate of heat transfer by measuring the Nusselt number for vertical as well as curved backward facing step.

3. The effect of expansion ratio has been studied on the reattachment length and Nusselt number for vertical as well as curved step.

1.4 Applications of current study

Such flows are widely implemented in many engineering and technological applications, some of which are as follows:

1. Sudden expansion devices
2. Heat exchangers
3. Combustion chambers
4. Cooling of electronic devices
5. Electrical rotating devices
6. Automobiles
7. Air foils

1.5 Organisation of thesis

The thesis comprises of five chapters followed by the references. The chapter 1 deals with the introduction which covers the basic flow behaviour past a backward facing step, need of the study, objectives of the present study and its applications. The chapter 2 deals with the literature review which covers the common features of the flow discussed in the previous investigation of the flow over a backward facing step. The chapter also includes the research work accomplished by the various authors for two dimensional and three dimensional vertical as well as curved backward facing step. The chapter 3 deals with the methodology adopted to carry out the numerical simulation to investigate the flow and heat transfer over a backward facing step. The methodology includes the modelling of the backward facing step and the corresponding mesh generation. The methodology also includes the numerical method, governing equations and the boundary conditions used for the numerical procedure. The chapter 4 deals with the results and discussions which cover the calculation of reattachment length and Nusselt number for two and three dimensional vertical as well as curved backward facing step. The results are obtained for wide range of Reynolds number covering laminar as well as turbulent flow and also for different expansion ratios. The results obtained for vertical step are compared with the curved step. The chapter 5 deals with the conclusion of the present study which summarises the whole investigation from introduction to results and discuss about the future scope of the present study.

Chapter 2

Literature Review

2.1 Introduction

A significant amount of literature has been reviewed and it was found that the maximum work has been done for analysis of flow structures that are formed downstream of the backward facing step. The literature available described the flow characteristics for the laminar as well as turbulent flow. The eminent researchers including Armaly et al. [1983] and Driver et al. [1987] carried out some earlier investigation into the flow behaviour downstream of backward acing step. Then a limited literature available for heat transfer was reviewed to study the parameters that affect the rate of heat transfer during the flow. The researchers conducted the earlier study on flow and heat transfer including Kondoh et al. [1993] and Nie et al. [2003]. The various researchers have analysed the flow past a backward facing step along with heat transfer for both laminar and turbulent flow. From the literature it was concluded that the flow over a backward facing step is affected by parameters like step height, channel height and Reynolds number. Due to its application in micro electromechanical systems this study is done for heat transfer point of view in recent years. The following section will discuss about the characteristics of backward facing step flow.

2.2 Common characteristics of backward facing step flow

The flow over the backward-facing step (BFS) comprises many critical phenomenon and instability mechanisms. The various characteristics of the flow over a backward facing step include the free shear layer, recirculation region, reattachment zone and rolling of vortices downstream of the step. Figure 2.1 shows all these important characteristics of the backward facing step flow found in the literature.

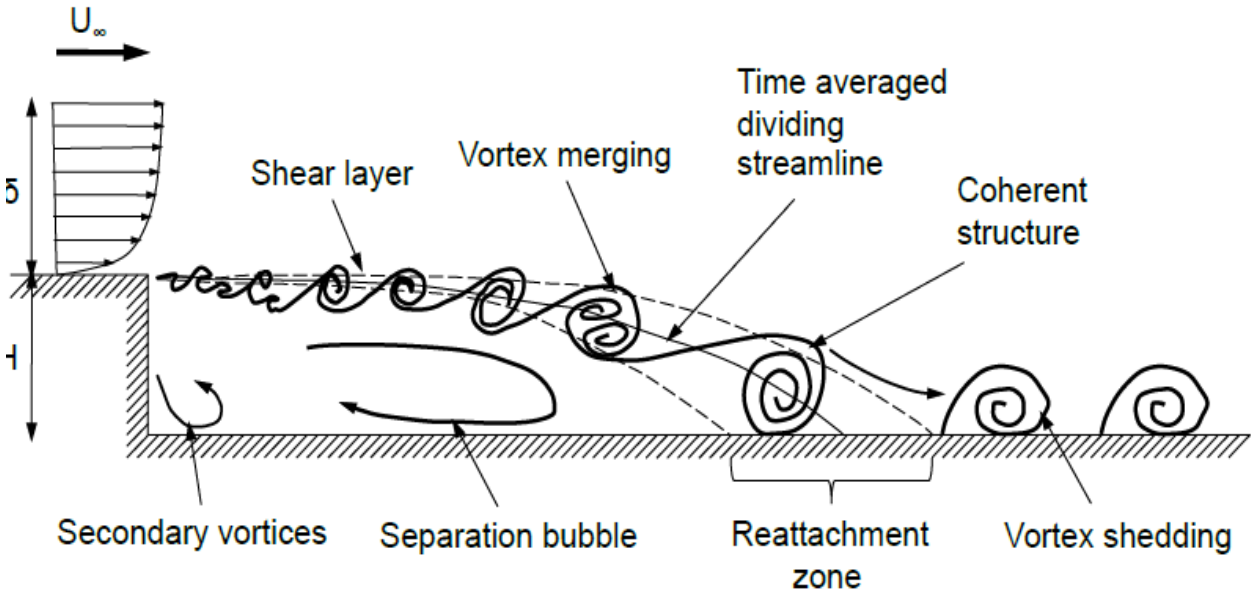

Figure 2.1: Flow characteristics behind BFS [Driver et al., 1987]

According to flow structures formed downstream the backward facing step the wake can be split into three regions namely shear layer region, recirculation region and reattachment zone. Initially for turbulent flow the boundary layer separates at the step due to the development of adverse pressure gradient during the flow, which leads to formation of thin shear layer. For turbulent flow by the aggregation of turbulent structures shear layer starts growing. The vortical structures contained in the fluid entrain the other fluid that is present outside the shear layer and due to which recirculation region is formed between the shear layer and adjacent wall. Due to prevailing of adverse pressure gradient condition downstream of the step the shear layer starts curving downwards and finally impinges on the wall and creates the reattachment point. The distance from the step to the reattachment point is called as reattachment length. As due to oscillating nature of shear layer it is not possible to define a particular reattachment point rather we define the reattachment zone. Hence these three regions control the flow past a backward facing step. We can also alter these characteristics of the flow to get the desired effect like to reduce the drag, noise, vibration and enhance the rate of heat transfer. N. Lancial et al. [2013] in a turbulent flow over the backward facing step accounting the heat transfer gave the correlation between the maximum heat transfer and maximum Reynolds number.

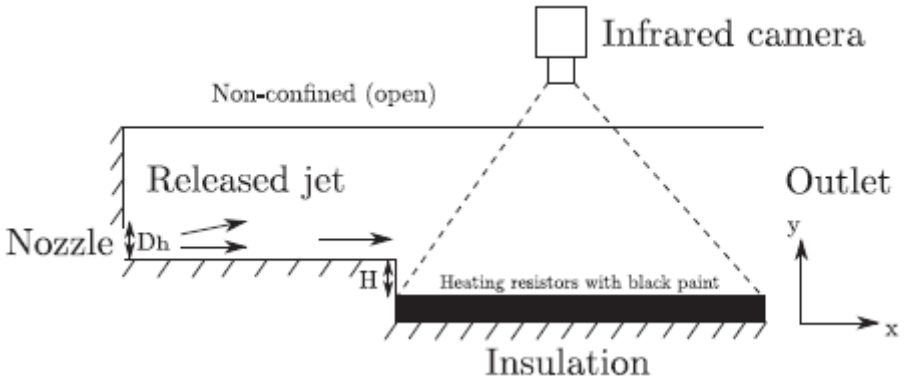

Figure 2.2: Closer view of studied region of flow [N. Lancial et al., 2013]

2.2.1 Shear layer region

The fluid layer containing the velocity gradients which lead to viscous shearing is called as shear layer. There can be two shear layers in the flow past a backward facing step, one is free shear layer and other is wall bounded shear layer. The free shear layer develops at separation point and then grows and finally reattaches on the wall surface. The free shear layer is developed due to velocity gradients present between the high momentum fluid and lower low momentum fluid present in the wake region or recirculation region. There are many instabilities prevailing in the free shear layer.

2.2.2 Rolling and pairing mechanism of vortical structures

The free shear layer comprises of rolling and fusion of vortical structures. The researchers found the prevailing vortex pairing mechanism in the free shear layer in the flow over a backward facing step. In the experiments conducted to analyse the vortex pairing mechanism, it was found that vortical structures formed in the shear layer are due to the combination of adjacent turbulent structures. The vorticity region leads to velocity gradients in the vertical direction which further leads to make the discrete vortical lumps and this process of developing vorticity lumps is known as rolling of vortices. The vortex pairing is the process of combination of adjacent vortical structures present in the flow. The adjacent vortices altogether lead to form the common vortex in the free shear layer and it keeps on growing until the free shear layer reattaches on the wall surface. The main factor that affects the growth of shear layer is merging of adjacent vortices as a result of vortex pairing mechanism. The free shear layer will goes on expanding until it comes across some obstruction or wall.

2.2.3 Vortex shedding mechanism

Kapiris et al. [2014] reported that the shedding instability were a common phenomenon in free shear layer flows. The study of shear layer before and after reattachment has been carried out by many researchers. They concluded that after reattachment the free shear layer develops into another shear layer providing a sub boundary layer. Vortex shedding during a flow leads to the oscillating motion when some fluid like air flows over a cylinder or any bluff body. The shedding instability prevailing during the backward facing step flow resembles the Von Karman vortex shedding. The growth of vortex in size is also attributed to merging of adjacent vortical structures along with the flow. Kevin Helmholtz instability has become the reason behind the growth of small scale vortices in the shear layer. The length scales attained by the vortical structures is found to be of the order of step height in backward facing step flow as compared to that of channel height in mixing layer flow.

2.2.4 Reattachment zone

The shear layer separating from the step and then reattaches at the surface. There is not a single fixed point for the reattachment of shear layer due oscillating nature of free shear layer. Therefore a reattachment zone is defined on the wall surface for shear layer. This fluctuating nature of shear layer is called as flapping of shear layer. Albeit many authors have described this phenomenon of flapping but still there is no persuading theory derived so far. It is also proposed that vortical structures present in the shear layer generates the pressure gradient in the recirculation region which further leads to higher recirculation and lesser reattachment length.

2.2.5 Recirculation zone

The region which is surrounded by free shear layer and the bottom wall is called as recirculation zone. The recirculation region is encouraged by entrainment of fluid from the recirculation region with the help of vortices present in the free shear layer. There are generally two kind of recirculation vortices seen during the backward facing step flow, one is primary vortex and other is secondary vortex. The primary vortex is present in the central region whereas the secondary vortex is confined near the corner of step as shown in fig. Earlier the instruments used to detect the flow in recirculation region were hot wires and Pitot tubes which produced significant inaccuracy. Later as the technology advanced the new

instruments like Laser Doppler Anemometer and PIV were used to extract the more accurate information about the flow in the recirculation region.

2.2.6 Flow separation

Figure 2.3 shows the flow separation and sufficient condition for flow to separate. Separation is the phenomenon which takes place when the fluid momentum near the surface is reduced to zero by the combined action of viscous and pressure forces. The necessary condition for flow separation to occur is that pressure gradient should be adverse ($\partial p/\partial x>0$). But this is not the sufficient condition. The sufficient condition for separation is that velocity gradient at surface should be equal to zero ($\partial u/\partial y=0$ at $y=0$). In case of turbulent boundary layer the momentum of fluid is higher than laminar boundary layer. Therefore the turbulent boundary layer is better able to resist separation in an adverse pressure gradient.

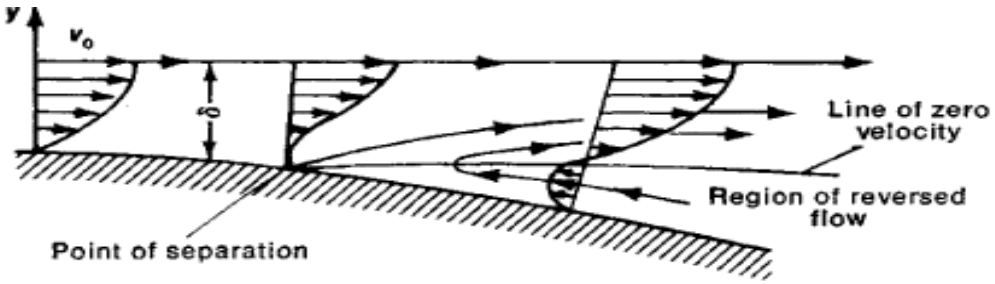

Figure 2.3: Flow separation phenomenon.

Boundary layer separation can occur for internal flows. It can result from such causes such as a rapidly expanding duct of pipe. Separation occurs due to an adverse pressure gradient encountered as the flow expands, causing an extended region of separated flow. The part of the flow that separates the recirculation flow and the flow through the central region of the duct is called the dividing streamline. The point where the dividing streamline attaches to the wall again is called the reattachment point. As the flow goes farther downstream it finally attains an equilibrium state and has no reverse flow.

2.2.7 Effects of flow separation

When the boundary layer separates, its displacement thickness increases abruptly which modifies the outside potential flow and pressure field. In the case of airfoils, the pressure

field modification results in an increase in pressure drag, and if severe enough that will also result in loss of lift and stalling, all of which are undesirable. For internal flows, flow separation enhances the flow losses, and stall-type phenomena such as compressor surge, both are undesirable phenomena. Another effect of boundary layer separation is vortex shedding, known as Karman vortex street. When the vortices begin to shed off the bounded surface they do so at a certain frequency. The shedding of the vortices then could cause vibrations in the structure that they are shedding off. When the frequency of the shedding vortices reaches the resonance frequency of the structure, it could cause serious structural failures.

2.2.8 Methods to prevent separation

1. Suction
2. Vortex generator

1. Suction:

There are many cases where the control of boundary layer separation is very important. Separation control by suction is achieved by drawing the low momentum layers from the bottom of the boundary layer into the suction slots. This draws the higher energy air from the outer high energy layers closer to the surface.

2. Vortex generator:

A vortex generator is a device that creates a swirl due to its shape. Vortex generators work by mixing high energy air from the free stream with the lower energy air found in the boundary layer. The vortices created by these generators cascades energy and momentum from the free stream to the boundary layer due to their swirling motion. In other words, the vortex generator increases the mean stream wise energy of the boundary layer by drawing in high energy fluid from the free stream. This process is called reenergizing the boundary layer. The higher momentum fluid is more resistant to separation and leads to higher performance of the aircraft.

2.3 Significance of Nusselt number

It is a dimensionless number which is defined as the ratio of convective to conductive heat transfer. Nu signifies the rate of heat transfer in a forced convective flow.

2.4 Parameters affecting the flow and heat transfer

The most commonly observed characteristics of the flow behind a BFS were discussed in the previous sections. Apart from the complexity involved due to the instabilities in the flow, the flow characteristics behind the step were also found to be dependent on certain flow and geometric parameters. The parameters that significantly affect this flow are the aspect ratio, expansion ratio, free stream turbulence intensity, Reynolds number, and the boundary layer state and thickness at separation as discussed by Yanhua Wu et al. [2013]. They studied the influence of individual parameters on reattachment length. Technological advancements in the instrumentation field and analytical schemes have make it possible to measure readily more information such as the coefficient of pressure, the turbulent structure characteristics in the shear layer, power spectral data, to name only a few. Nonetheless, the reattachment length is used in the following discussion as the primary parameter of comparison since it is the most commonly reported parameter in previous studies.

2.5 Definition of meshing quality parameters

The meshing parameters are defined to check the quality of mesh. There are mainly three parameters namely skewness, aspect ratio and orthogonal quality that will be defined in the following section.

1. Skewness

Skewness is the measure of difference between the cell and the equilateral cell possessing equivalent volume. The higher value of the skewness will lead to less accuracy and destabilisation of the solution. According to the general rule for triangular and tetrahedral mesh the value of skeweness should be kept below 0.95 otherwise it will lead to convergence difficulties.

2. Aspect Ratio

Aspect ratio measures the stretching of the cell. For the stability of the flow the aspect ratio may go as high as possible but for energy stabilisation purpose the aspect ratio should be kept below 35.

3. Orthogonal Quality

The orthogonal quality is measured by using face normal vector which is drawn from the cell centroid to the centroid of each adjacent wall and vector drawn from cell centroid to each of the faces. The orthogonal quality lies between 0 and 1. The desirable value of orthogonal quality should be close to 1.

2.6 Previous research work

The literature based on previous work carried out on analysis of fluid flow and heat transfer over the vertical and curved backward facing step has been studied and presented in the following text.

2.6.1 Literature for 2-D vertical backward facing step

There is plenty of literature available for two dimensional vertical backward facing step. The various researchers have studied the flow and heat transfer characteristics over a vertical backward facing step which is described as under.

Armaly et al. (1983) conducted the experimental study of the flow over two dimensional backward facing step with the help of Laser-Doppler anemometer for analysing the velocity distribution and reattachment length. The working fluid used was air. The expansion ratio taken was 1:1.94. The test section was constructed from aluminium. The dimensions of the geometry were kept as to ensure the fully developed flow. The study has been performed for Reynolds number range of 70 to 8000. The variation of the reattachment length was seen against the Reynolds number. Apart from the primary recirculation region there were other recirculation regions seen downstream of the backward facing step both at the top and bottom of the channel. The experiments showed that the flow remains two dimensional for low and high Reynolds number. The results obtained are also compared with the numerical results computed by solving the conservation equations for mass and momentum. The experimental results were found in good agreement with the numerical results.

The two dimensionality of the flow was found to be justified for the range 400>Re>6000. In the mean range the flow character was found to be strongly three dimensional. The velocity profile seen at the step found close to parabolic. The investigation found out that after the Re = 6600 the reattachment length remains almost constant which was found in good agreement with the previous literature. In the range of Reynolds number

1200 to 2300 the second recirculation region was seen at the bottom wall downstream of the step. This region comprises of relatively small volume and velocity. The three dimensional behaviour of the flow was found to be accelerated with Reynolds number. In the numerical investigation the flow was found to turn from laminar to transition for Re = 1250. The reattachment length near the step was found to be highly dependent on the Reynolds number. A separation region found on the wall opposite to step disappears for highly turbulent flow. It was also found out that the vortices started appearing for Re = 800 and becomes dominant around Re = 2300 and disappeared for Re = 5000.

Kondoh et al. (1993) carried out the computational study for laminar air flow downstream of backward facing step in 2D. They conducted the calculations for different values of Reynolds number and expansion ratios. Reynolds number range was taken as 20, 50, 100, 200, 500 and for expansion ratio 1.25, 1.5, 1.67 and 2. The results obtained show that there was an increase in Nusselt number with increase in Reynolds number and expansion ratio. They also calculated the reattachment length for the flow which was found at X/S = 6.2 while experimentally it was calculated at X/S = 6. The downstream bottom wall is heated at constant temperature while other walls are kept as adiabatic. The influence of Prandtl number is also studied on the flow characteristics and heat transfer. For low Prandtl number the temperature profile is regulated primarily by conduction. For high Prandtl number the increase in the rate of heat transfer is seen significantly.

Chen et al. (2005) carried out the investigation to study the two dimensional incompressible steady flow with convective heat transfer over a backward facing step using Lattice Boltzmann Method. A square block is also inserted into the downstream flow region. The maximum value of Reynolds number taken is 200. The inlet velocity is fixed at 0.05. In boundary conditions for the wall Neumann and Dirichlet boundary conditions are applied. For Dirichlet boundary condition the constant temperature is applied on the wall and for Neumann boundary condition the constant heat flux is applied at the wall. The downstream wall is heated at constant temperature which is greater than the inlet temperature of the fluid while all other walls are kept as adiabatic. The recirculation region was found after the step. The reattachment points are found at X/h = 3.18 and 5.5 corresponding to Reynolds number 100 and 200 respectively. The reattachment length was found to increase with Re. The other recirculation region is also seen after the blockage. The Nu is found to increase with increase in Re. The peak of Nu is found to shift downstream with Re as the reattachment point

changes with Re. The heat transfer was observed to be more in case with blockage as compared to the case without blockage.

Chen et al. (2006) conducted the simulation of turbulent convection flow over a backward facing step and studied the effects of step height on the flow behaviour and heat transfer. Reynolds number and duct downstream length were kept at constant. A constant heat flux of 270 W/m^2 is applied at the stepped wall while the other walls are kept as adiabatic. The primary and secondary recirculation region increases with the increase in step height. The bulk temperature found to be increased with increase in step height. The increase in the step height leads to increase in maximum turbulent kinetic energy. In recirculation region there is no reasonable increase in coefficient of friction with step height. The magnitude of friction coefficient becomes smaller with increase in the step height. The maximum value of Stanton number decreases with increase in step height. It was observed that maximum turbulent kinetic energy prevails near the reattachment region and along the free separated shear layer. The length of flow recovery becomes more for increasing step height.

Kanna et al. (2007) carried out the investigation to study the conjugate heat transfer for incompressible flow over 2-D backward facing step. The analysis was done with the help of stream vorticity equations and energy equations for both fluid and solid part. The minimum value for Nusselt number was obtained after the reattachment region. The temperature value for interface was found decreased with increasing Reynolds number and also with increase in Prandtl number. The first peak for Nusselt number was seen near the inlet region due to entrainment of fluid and the second peak was found after the reattachment zone. The average value of Nusselt number for non conjugate case was found 12.12% higher compared to conjugate case for Re = 600. The increase in the conductivity leads to make the value of average Nu almost close for both conjugate and non conjugate cases.

Erturk (2008) conducted the numerical study of 2-D laminar and incompressible flow past a backward facing step. The governing equations for mass and momentum are solved using Finite Difference Method. The study has been performed for high Re. The results obtained are compared and found in good agreement with prevailing numerical and experimental literature. The length of the channel upstream of the step is 20 times the step height and length downstream of the step is 300 times the step height. The flow at inlet is assumed as fully developed having parabolic profile. The investigation of the flow is done up to Re = 3000. The size of the recirculation region found to increase almost linearly with Re. The three

recirculation regions were seen, one at the top wall and two at the bottom wall. The third recirculation region was seen on the bottom wall at around Re = 1800. The reattachment lengths both at the top wall and the bottom wall are plotted against the Re. The reattachment length was found to increase with Re.

Lima et al. (2008) presented the numerical study of three recirculation zones in the unilateral sudden expansion flow for 2D laminar flow. The two CFD codes are used for the analysis of flow characteristics. The results are calculated for Re < 2500. The governing equation for the fluid like mass conservation and momentum conservation is solved using finite element method and finite volume method. The results obtained numerically are compared and found in good agreement with the experimental results. The reattachment length was found to vary non-linearly with the Re. The expansion ratio is taken as 1.94. The x-y coordinate is set to zero at the corner of the step. The simple algorithm is used for velocity-pressure coupling. The analysis is done by taking quadrilateral element for FVM and triangular element for FEM. The three reattachment region forms on the downstream wall, two at the bottom and one at the top. The reattachment length is calculated as the function of Re and cell size. The three dimensional behaviour was observed around Re = 400 and transition region is seen around Re=1200. The recirculation region is detected at the top wall for Re = 648. The third recirculation region is found at the bottom wall for Re around 2000.

Velazquez et al. (2008) carried out the investigation for heat transfer enhancement downstream of backward facing step for laminar flow using pulsating jet. In this study the effect of two parameters namely velocity pulsation frequency and pressure gradient amplitude on the rate of heat transfer. The working fluid considered is water. The viscosity and conductivity are assumed as temperature dependent. The whole investigation is performed for unsteady case and the results obtained shows that the value of Nusselt number downstream of the backward facing step for unsteady case is always more than in the case of steady. For Reynolds number 100 and flow pulsating frequency is set at resonance frequency and the time averaged Nu measured downstream of the step is found to be about 55% more than the steady case. If we move away from the resonating frequency the time averaged value of Nu found to be decreased and finally reaches its value as that in steady case. The working fluid water is made to enter at 293K and downstream stepped wall is maintained at 353K. The value of Nusselt number was found to be more for higher pressure gradient amplitude for a particular value of frequency. The Nusselt number was found to be decreased for both

lower and higher value of forcing frequency. The periodic changes occurred in the flow lead to increase of Nusselt number in the recirculation region. It was also observed that heat transfer enhancement is more when viscosity and thermal conductivity of water are assumed as temperature dependent.

Rouizi et al. (2010) conducted the study to develop the reduced model to study the heat transfer applications with the help of Modal Identification Method. The problem studied in this investigation is forced convection two dimensional laminar flow over a backward facing step. The properties of the fluid are assumed as temperature independent. Hence the velocity can be considered as independent of temperature. The unsteady heat flux density is applied on the wall upstream of the step. The three reduced models that are studied in this paper are steady fluid mechanics, unsteady heat transfer for a given Re and unsteady heat transfer for Re in the range of 100 to 800. The expansion ratio taken is 2 and the upstream length of the channel is 1 cm. The step height is also considered as 1 cm. The working fluid taken is air which is considered as incompressible and Newtonian. The Fluent model of the Computational Fluid Mechanics is used to conduct the simulation. The developed reduced models were found to agree with detailed models and thus very helpful to reduce the computation time.

Terhaar et al. (2010) studied the laminar unsteady heat transfer over a backward facing step experimentally. The inlet flow is made as pulsated. The working fluid taken is water. The Reynolds number used based on the average velocity is 300. The temperature of the inlet fluid is kept constant at 30^{o}C while the downstream wall is heated up to the temperature of 74^{o}C. The piston pump is used to carry out the pulsation in the inlet flow and range of pulsation is studied up to Strouhal number of 1.2. The results verify the more efficiency of heat transfer in the pulsating case as compared to the steady case of backward facing step. The relation between the Nusselt number and Strouhal number is also seen. The Nusselt number is found to increase with Strouhal number up to a particular value after that it starts decreasing with increase in Strouhal number. The experimental results also confirm that there is no effect of pulsation on heat transfer for flow in a straight pipe. It also signifies that the extent to which pulsation frequency affects the heat transfer will depend on the geometry under consideration.

Hattori et al. (2012) presented the investigation of the heat transfer for turbulent flow in a turbulent boundary layer using Direct Numerical Simulation. For analysing the flow

characteristics and the heat transfer the two dimensional block is considered. The regions that are formed downstream of the block are studied like separation and reattachment. The effect of Reynolds number and the size of block is seen on the reattachment length and Stanton number. The reattachment length and Stanton number are found to increase with Re and decrease with width of the block with single exception. The vortices signifying the turbulent structures are clearly seen and their correlation is made with temperature gradient. The instant fluctuating flow profile is also seen very clearly. In this paper the quadrant analysis of the turbulent heat transfer is also carried out.

Togun et al. (2013) analysed the heat transfer and flow behaviour over a double backward facing step. The working fluid taken is air. The meshing and solutions are done using ANSYS CFD Fluent. The k-epsilon standard model is used to encounter the flow with separation and recirculation. The Reynolds number is varied from 98.5 to 512. The bottom downstream wall is heated at constant flux q=2000 W/m^2 while all other walls are set to adiabatic. The results obtained show that Nu increases with Re for all cases. The maximum value of Nu is obtained near the first step as compared to second step. Increasing the height of the channel downstream of the step lead to decrease of Nu while keeping the pattern of the profile same. The recirculation region is shown by stream line contours. The increase in the Nu is observed with decrease in step height.

Togun et al. (2014) presented a numerical study of heat transfer to turbulent and laminar Cu/water flow over a backward-facing step. Mathematical model based on finite volume method with is used to solve the continuity, momentum, energy and turbulence equations. Turbulence was modelled by the shear stress transport k-w Model. The effect of expansion ratio was clearly seen at the downstream inlet region where the peak of the Nusselt number profile was referred to as enhanced heat transfer due to the generated recirculation flow. The rise of pressure drop was found with an increase in Reynolds number. Generally, the highest pressure drop was observed at the downstream inlet region due to recirculation flow which caused the enhancement of heat transfer. A shear stress transport k–w Model with Reynolds numbers ranging from 50 to 200 for the laminar regime and 5000 to 20,000 for the turbulent regime, at a constant heat flux of 4000W/m2 and the expansion ratio fixed at 2, was taken. Calculations show that the heat transfer accelerated when the Reynolds number was increased. The maximum heat transfer increase was obtained for Reynolds number of 20,000.

2.6.2 Literature for 2-D curved backward facing step

A very few literature is available for flow and heat transfer analysis over two dimensional curved backward facing step which is described as under.

Ratha et al. (2014) studied the flow past a backward facing step incorporating vertical as well as curved step numerically. The working fluid used for the study is air. The reattachment length is calculated for wide range of Reynolds number covering laminar to turbulent flow including the transition flow regime. The investigation of flow and reattachment length is also carried out for different expansion ratios ranging from 1.24 to 2.20. During the study of flow over backward facing step the two recirculation regions are observed, one at the bottom wall called as primary recirculation zone and another at the top wall called as secondary recirculation zone. The reattachment length is calculated for primary recirculation zone as well as secondary recirculation zone. The laminar flow regime was observed for the Reynolds number up to 900. The reattachment length was found to increase with increase in the Reynolds number for laminar flow. The reattachment length is also found to increase with increase in the expansion ratio. It is also observed that the secondary recirculation zone prevails only for laminar and transition flow regimes.

2.6.3 Literature for 3-D vertical backward facing step

A sufficient amount of literature is available for heat transfer and flow analysis of three dimensional vertical backward facing step. The different authors have studied the flow behaviour past a backward facing step by calculating the reattachment length and Nusselt number for heat transfer analysis. The different literature found for 3-D vertical backward facing step is described as under.

Barkley et al. (2002) reported the computational stability analysis for the flow over three dimensional backward facing step. The expansion ratio considered is 2 and the aspect ratio is 37. The Reynolds number range is taken from 450 to 1050. The primary instability that occurs during the flow is for Re just below 750. The study identified that the flow remains stable up to Re = 1050. The dependence of eigen values on the Re is shown. The investigation revealed that the eigen values will approach zero as the Re approaches infinity. The limit of Re up to which this study is conducted no instability in two dimensional flow is seen. The results obtained are compared and found to be validated with Armaly et al. (1983). In both studies Re = 300 is selected to define the boundary between the two dimensional and

three dimensional behaviour of the flow. It is also stated that Re = 300 cannot taken as fixed critical point. The observations also revealed that side walls play important role in the three dimensional behaviour of the flow. The reason behind the development of secondary flow region with separation is attributed to centrifugal instability.

Nie et al. (2002) conducted the simulation to study the convective flow past a three dimensional backward facing step and studied the effect of different step heights. The research was performed for constant value of Re = 343. The constant heat flux ($q = 50W/m^2$) condition was enabled for downstream bottom wall while all other walls were kept adiabatic. The expansion ratio was kept constant at 2. The size of the primary recirculation zone was found to be increased with increase in the step height. The maximum value of Nusselt number was found in the region where the reattachment length was found as minimum. The maximum value for the coefficient of friction was found to be proportional to the step height in the recirculation region and the case was reversed for the region after the reattachment. The three dimensional characteristics and side wall effects were found to be increased with increasing step height. The reverse flow regions were attributed to the development of adverse pressure gradients in the flow when flow separated from the step. There was also the jet like flow seen in the separated shear layer adjacent to the side wall. The maximum value for reattachment length was found for the side walls rather than the centre of duct as usually expected. Reverse flow regions were found to be increased with increasing step heights near the side walls. The maximum value for Nusselt number was found increased with increase of step height and it shifted further downstream.

Nie et al. (2003) studied the reattachment of the flow over a three dimensional backward facing step. The analysis was carried out to study the flow behaviour on the adjacent wall along with the heat transfer. The heating source was provided at the bottom of the downstream wall and other walls were set to adiabatic. The flow behaviour was studied for Re=400, they found the usual recirculation region near the step and also vortex was formed along the adjacent side wall over the span. A jet like flow was seen moving towards the step and then redirects to the side wall. The maximum rate of heat transfer was attributed to jet like flow that strikes the stepped wall. The stream lines were shown for the flow along side walls and velocity components in all x, y and z directions were plotted. The variation of the Nusselt number was also seen with the length of the heated wall. There was sudden increase in the Nusselt number in the recirculation region due to formation of the turbulent structures.

Biswas et al. (2004) studied the three dimensional backward facing step flow for various expansion ratios for low and moderate Reynolds numbers. The expansion ratios used were 1.94, 2.5 and 3. The results obtained show that the flow remains two dimensional for the Re up to 400. The reattachment was found to be increased with Reynolds number. The pressure coefficient was found to vary inversely with Reynolds number. The pressure drop had also been calculated for the backward facing step flow for different values of Re. It was found that higher expansion ratios lead to greater pressure drop. The results implied that the three dimensional flow behaviour was observed at ER = 1.94 for Re greater than 400. A wall jet like characteristic was observed for the flow having Re > 400. For lower Re the corner vortex is formed which transforms into recirculation region for higher Re. The losses that are adding to frictional losses in pressure drop found to be increased with increasing step height and decreasing with increase in Re.

Saldana et al. (2005) conducted the numerical study for mixed flow past a three dimensional backward facing step. The downstream wall was maintained at constant temperature while all other walls were maintained as adiabatic. The geometry considered in this study has AR = 4 and ER = 2. The finite volume technique was used to carry out the simulation work. The flow at the inlet was assumed to be fully developed and isothermal. The step was treated as conducting block. The variation of Nusselt number was obtained against the stream wise direction and along the span wise direction. It was observed that buoyancy forces are of great importance for mixed convection flows. The decrease in the primary recirculation region was observed with increase in Richardson number. For mixed flow the fully developed flow condition was not achieved at the exit. The magnitude for vertical velocity component v was found less near the top and bottom walls. The higher value for v was obtained where the buoyancy effect dominated.

Rani et al. (2007) carried out the investigation to study the eddy structures formed during the transitional flow downstream of backward facing step. The expansion ratio taken is 2.02 and aspect ratio is 8. The Re considered is 1000 and 2000. The step height is taken as 1 cm and upstream height of inlet channel is considered as 0.98 cm. The length of the channel taken is $-150 < X/S < 75$. The y and z component of velocity are set to zero at inlet. The eddy present in the vicinity of the step lead to Kelvin-Helmholtz stability which is found to be accelerated by higher Re. The instabilities made the shear layer to roll up which further triggers the flow to become turbulent from transitional phase. For Re = 2000 the vortices are found to move

from side walls to the centre and hence more instability was observed in the central plane. In the current study which is focussed more on the roof eddy revealed that the roof eddy is more unstable as compared to the floor eddy. The instability was found dominating in the free shear layer. It is concluded that the higher Re is required to have the instabilities and vortices downstream of backward facing step.

Tinney et al. (2009) conducted an experimental study to investigate the flow over 3-D backward facing step. The investigation is performed using an instrument called PIV and also combining with oil flow visualization. The inlet flow velocity used is 10.4 m/s corresponding to the Reynolds number 9000. The present study only deals with zero angle of attack. The results obtained tell about the horse shoe vortex prevailing after the step. A very high amount of perturbations are found in the central region of channel and these are much higher as compared to 2-D back step. The results also show the contours of turbulent shear stresses. The observations also show the anti clockwise vortex pair rotating just after the saddle point. The perturbations found in case of three dimensional case are much higher than in the case of two dimensional.

Oztop et al. (2012) conducted the study to analyse the turbulent flow and heat transfer over double forward facing step with obstructions. The inlet flow temperature is maintained constant at 293 K and the bottom wall and the steps are kept at 313 K. The shape of the obstacles is chosen to be of rectangular cross section and placed upstream of each step. The mathematical equations like mass conservation, momentum conservation and energy conservation are solved using finite volume technique. For encountering the turbulent flow the K-epsilon modelled is used. The effect of step height, aspect ratio and Re is seen on the flow and heat transfer characteristics. The results obtained show that there is increase in the heat transfer with increase in aspect ratio of obstacle. The pressure drop was found to increase with aspect ratio. The study is performed for the Re range from 30000 to 100000. The maximum Nusselt number is found for AR = 1. The maximum value for Nu is obtained somewhere near the second step. The increase in Nu is seen with increase in Re and step height due to development of recirculation region more severely for higher Re. The least value for the pressure coefficient is observed near the second step.

Lancial et al. (2013) studied the effect of turbulent wall jet on the heat transfer characteristics during the flow downstream of non confined backward facing step both experimentally and numerically. The effect of inlet flow and step height has been seen on the

flow and heat transfer. The infrared camera is used to draw the temperature profile and hot wire approach is used for measuring the instantaneous velocity. The skin friction coefficient is calculated to the flow characteristics and Nu is calculated to estimate the heat transfer during the flow. The significance of Nusselt number lies in the fact that it enables us to compare the convective heat transfer with conduction heat transfer. A correlation is also presented for maximum Re and maximum Nu. The fan used to generate the velocity in the range from 0 to 19.62. An electrical transformer is used to provide the heating of the downstream step and the temperature of the wall is limited to 70^{o}C. The numerical analysis is performed using the computational fluid dynamics. The k-omega SST model is used to encounter the turbulent flow. The higher the step height and Re higher will be the reattachment length.

Wu et al. (2013) carried out the experimental investigation to study the turbulent flow over a rough backward facing step. The study is carried out to analyse the effect of rough surface and smooth surface on the turbulent flow. The rough surface is chosen as practically there is a film deposition of the foreign material. To see the flow profiles both in x and y direction the high resolution PIV instrument is used. The Reynolds number based on the average inlet velocity is taken as 3450 and expansion ratio of 1.01. The ratio of boundary layer thickness to the step height is fixed at 8. The reattachment length is measured depending on the roughness of the channel. For some roughness value the reattachment length is found to be more and at some other positions it is found to be decreased with roughness. The observations carried out tell that roughness provided decreases the disturbance in the flow caused by the step. The study also concluded that the roughness lead to decrease the turbulence in the free shear layer. The observations also revealed that there is flow separation even before the step due to roughness prevailing. The effect of the roughness lessens on the Reynolds stresses as we go away from the step. The roughness also affects the Reynolds normal stress up to a certain distance from the step that is x/h = 5.5 after which affect is very small. The vorticity present in the recirculation region is seen to be affected by roughness of the surface.

Gautier et al. (2014) carried out the experimental study to control the recirculation area downstream of the step by providing an pulsating jet upstream of the step. The effect of duty cycle, frequency and amplitude of the pulsating jet is computed on the recirculation region. The two values of Re considered during investigation are 2070 and 2900. The working fluid used is water. The height of the backward facing step is h = 1.5 cm, channel height H = 7 cm,

channel width w = 15 cm, expansion ratio ER = 0.82 and aspect ratio AR = 1.76 cm. The pulsation is provided by a slot jet. The decrease in the recirculation area is observed as maximum when pulsation frequency is made equal to vortex shedding frequency. The recirculation area is also found affected by Kelvin Helmholtz instabilities prevailing in shear layer. The recirculation area was found to increase with amplitude of pulsating jet. In particular cases the recirculation area found to be reduced to null while reattachment length remains significant.

Kapiris et al. (2014) conducted the experimental study for analysing the vortical structures downstream of backward facing step when inlet flow is periodically perturbed. The working fluid used is air. The instrument used is PIV to measure the instant velocity fluctuations. The Reynolds number taken is 6940. The Strouhal number is varied from 0.026 to 0.23. The results revealed the decrease of 20% in the reattachment length. Due to combination of the newly formed vortices with the prevailing one the size of the separation bubble decreases. The effect of the pulsation frequency was also seen on the reattachment length. The pulsating frequency is varied from 1.66 Hz to 14.28 Hz. The both clockwise and counter clockwise vortices are captured in snap shots. The maximum reduction in reattachment length was found corresponding to Sth = 0.16.

Chapter 3

Methodology

3.1 Introductory comments

Flow over a backward facing step along with heat transfer is studied for both two dimensional and three dimensional cases using ANSYS Fluent. The analysis of flow and heat transfer is carried out for laminar as well as turbulent flow. The study conducted also includes the calculation of reattachment length and Nusselt number for curved backward facing step. The grid independency test is performed for all cases before running the numerical simulation. The geometry is modelled in the ANSYS Fluent for both two dimensional and three dimensional backward facing steps. After that the mesh is generated with the proper element size obtained from the grid independency test. The required boundary conditions are provided at the inlet, outlet and on the walls. The second order upwind method is used for solving the energy and momentum equations.

The governing equations used for the numerical study of flow and heat transfer are based on the conservation of mass, momentum and energy. The governing equations are solved in the Fluent using finite volume method which involves discretization and integration of governing equation over the control volume.

3.2 Two dimensional backward facing step

Due to lack of complexity in analysing the flow and heat transfer many authors have preferred to study the flow over 2-D backward facing step. In the current study the geometry of 2-D backward facing step is taken according to Kondoh et al. [1993]. The following sections will deal with description of geometry, governing equations boundary conditions and numerical procedure.

3.2.1 Problem description

The present study considers the numerical simulation of the two dimensional incompressible laminar flow of air along with heat transfer over a backward facing step. Figure 3.1 shows the geometry along with its parameters of the backward facing step as considered in Kondoh et al. [1993]. The length of the flow upstream to the step is 10 times the step height and the

length of the flow downstream to the step is 50 times the step height. The x, y coordinates are set to zero at the bottom of the step. The flow behaviour and heat transfer characteristics are studied at various Reynolds numbers of 50, 100 and 200. Also the flow and heat transfer characteristics are studied for various expansion ratios of 1.5, 1.67, and 2. The downstream bottom wall is heated at constant temperature while all other walls are set to adiabatic. The temperature of wall downstream of the step (T_w) is kept 10^o C higher than the fluid temperature (T_f) at inlet.

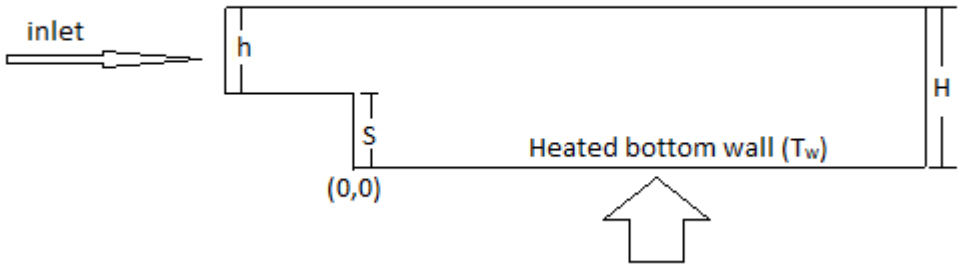

Figure 3.1: Schematic of 2-D vertical backward facing step

Similarly, the present study also deals with the analysis of flow and heat transfer over a two dimensional curved backward facing step. Figure 3.2 shows the geometry for 2-D curved backward facing step. The investigation is carried out for radius of curvature 0.007m. The analysis is performed for wide range of Reynolds number covering laminar as well as turbulent flow. The dimensions of step height, upstream and downstream length of the back ward facing step is similar to vertical backward facing step shown in Fig 1.

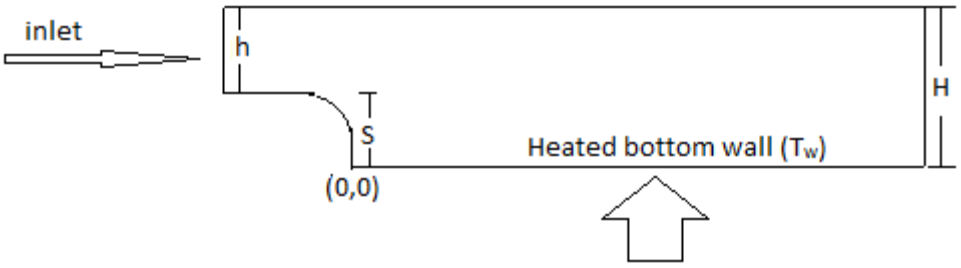

Figure 3.2: Schematic of 2-D curved backward facing step

3.2.2 Mesh generation

The mesh generated for the vertical backward facing step geometry shown in the Fig. 3.1 is represented in Fig 3.3. Similarly, the mesh generated for curved backward facing step geometry shown in Fig. 3.2 is represented in Fig. 3.4. The mesh is generated using ICEM software in ANSYS. The quadrilateral elements of size 0.0015 m is chosen to generate the mesh for vertical backward facing step and elements of size 0.0012 m is chosen to generate the mesh for curved backward facing step .

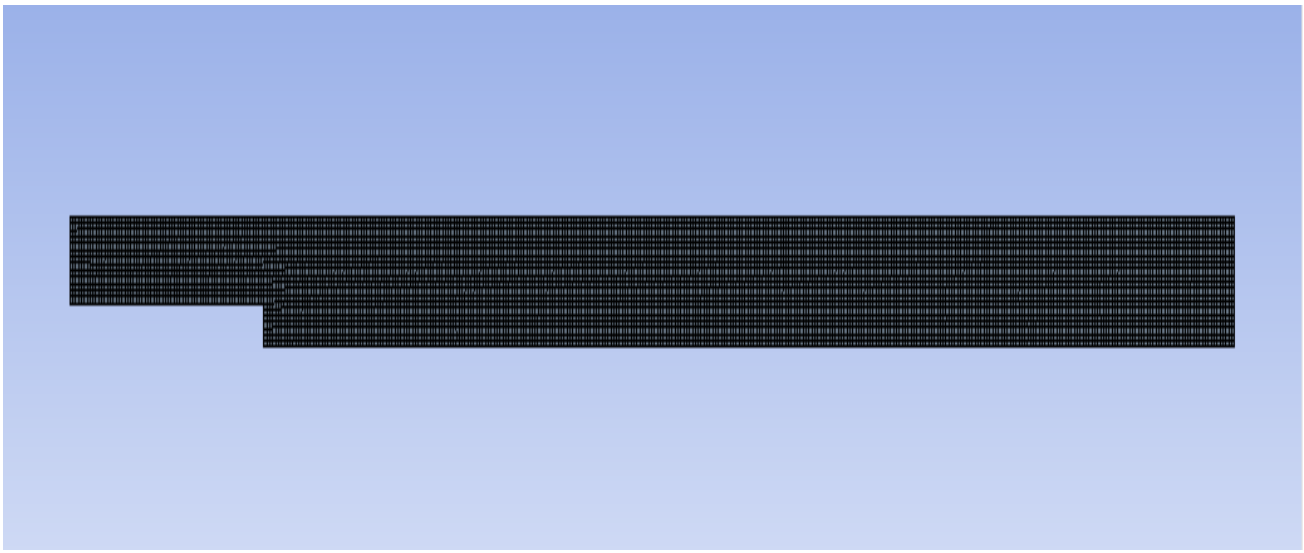

Figure 3.3: Grid generation for 2D vertical backward facing step with quadrilateral element.

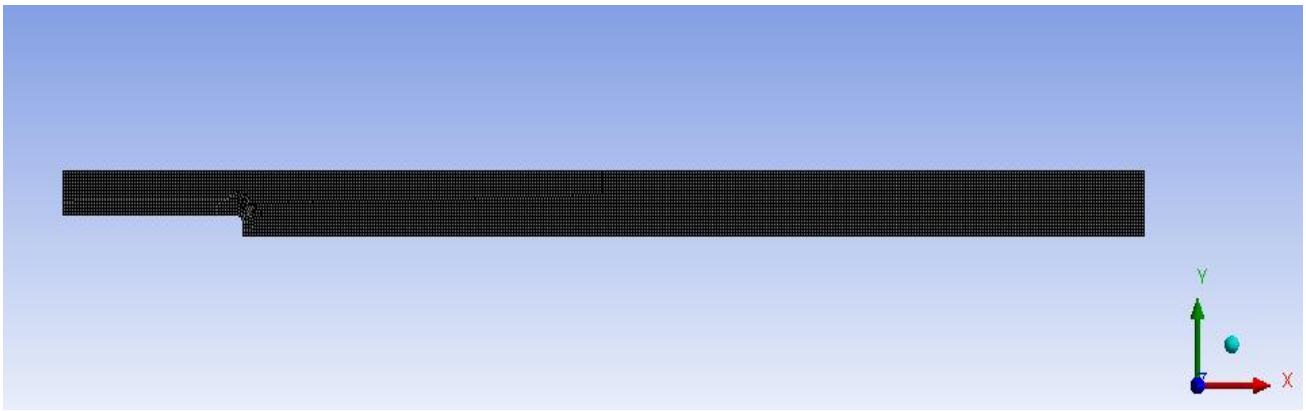

Figure 3.4: Grid generation for 2-D curved backward facing step

3.2.3 Meshing quality parameters

The accuracy of the results obtained from a numerical simulation generally depends on the quality of the mesh. The various mesh quality parameters are checked for the mesh generated in the geometry in order to ensure its quality. Table shows the various mesh quality parameters obtained for the mesh created for vertical backward facing step and it is found that all the parameters are lying within its limiting values.

Table 3.1: Meshing quality parameters for 2-D vertical step

Parameter	value	Limiting Value
Maximum Skewness	0.072	< 0.95
Maximum Aspect Ratio	1.068	< 35
Orthogonal Quality	0.99	Close to 1

Similarly, Table 3.2 shows the various mesh quality parameters obtained for the mesh created for curved backward facing step and it is found that all the parameters are also lying within its limiting values.

Table 3.2: Meshing Quality Parameters for 2-D curved backward facing step

Parameter	value	Limiting Value
Maximum Skewness	0.4	< 0.95
Maximum Aspect Ratio	1.75	< 35
Orthogonal Quality	0.99	Close to 1

3.2.4 Numerical procedure

ANSYS FLUENT software is used to carry out the numerical simulation. The pressure based solver along with viscous laminar model is chosen to solve the continuity equation, X-Y momentum equation and energy equation. The SIMPLE algorithm is used for solving the Navier-Stokes equations.

3.2.5 Governing equations

The continuity equation, X-Y momentum equations and energy equation are used as governing equations for the numerical simulation of two dimensional backward facing step are represented in Eq. 1-4.

$$\frac{\partial u}{\partial x} + \frac{\partial v}{\partial y} = 0 \quad (3.1)$$

$$u\frac{\partial u}{\partial x} + v\frac{\partial u}{\partial y} = -\frac{\partial p}{\rho \partial x} + \nu\left(\frac{\partial^2 u}{\partial x^2} + \frac{\partial^2 u}{\partial y^2}\right) \quad (3.2)$$

$$u\frac{\partial v}{\partial x} + v\frac{\partial v}{\partial y} = -\frac{\partial p}{\rho \partial y} + \nu\left(\frac{\partial^2 v}{\partial x^2} + \frac{\partial^2 v}{\partial y^2}\right) \quad (3.3)$$

$$u\frac{\partial T}{\partial x} + v\frac{\partial T}{\partial y} = -\frac{\partial p}{\rho \partial y} + \alpha\left(\frac{\partial^2 T}{\partial x^2} + \frac{\partial^2 T}{\partial y^2}\right) \quad (3.4)$$

3.2.6 Boundary conditions

The boundary conditions are used for the solutions are as follows:

- At inlet: u = u_{in} and v=0, T_f =300K
- At outlet: Gauge pressure=0
- At walls: walls are kept stationary and with no slip condition. The heated wall is maintained at constant temperature while others are insulated.

Table 3.3 shows the various properties of air considered for the present study.

Table 3.3: Properties of air used for numerical simulation

Properties	ρ (Kg/m^3)	C_p (KJ/kgK)	μ (Kg/m-s)	K (W/mK)
Air	1.225	1006.43	1.7894e-05	0.0242

3.2.7 Convergence criteria

Table 3.4 shows the convergence criteria specified for continuity equation, x-velocity, y-velocity and energy equation for the present numerical solution of backward facing step.

Table 3.4: Convergence criteria for 2-D laminar flow

Parameter	Convergence Criteria
Continuity	0.001
X-Veocity	0.001
Y-Velocity	0.001
Energy	1e-06

3.2.8 Under relaxation factors

Table 3.5 shows the under relaxation factors used for different parameters involved in the numerical solution of flow and heat transfer over the backward facing step.

Table 3.5: Under relaxation factors used for the present simulation

Parameter	Value
Pressure	0.3
Density	1
Body forces	1
Momentum	0.7
Energy	1

3.2.9 Grid independency test

The grid independency test is performed to make the results independent of the grid size after a particular number of elements. The present study considers three different cases for the grid independency test. The vertical backward facing step with expansion ratio 1.5 is discretized into 2218 elements for case 1 and then it is made finer by discretizing into 7531 and 12027 elements for case 2 and case 3 respectively. The model is simulated using governing equation represented in Eq. (3.1) to (3.4) along with the boundary conditions represented in section 3.2.6. The properties of air, convergence criteria and under relaxation factors represented in Table (3.3) to (3.5) are also used for the numerical simulation for all the three different cases. The nusselt number is determined for all the three different cases for Reynolds number 100. Figure 3.5 shows the variation of Nusselt number with the

distance from the step normalised by the step height. It is found from Fig. 3.5 that there is a significant change in the peak of nusselt number when the number of elements are increased from 2218 to 7531 but the change in results are insignificant for further increasing the number of elements in domain from 7531 to 12027. Also the average value of Nusselt number is calculated on the heated downstream wall for all the three cases. Table 3.6 shows the average nusselt number on the heated downstream wall and it is found that the change in the value of average Nusselt number is almost insignificant when the number of elements is increased from 7531 to 12027.So the optimum number of element is found to be 7531 which is used further for numerical simulation.

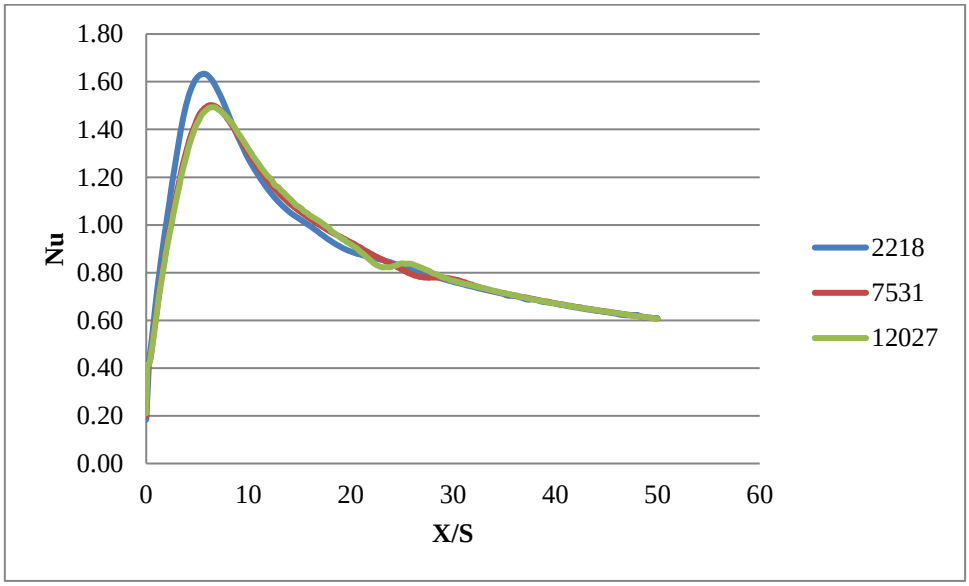

Figure 3.5: Grid independency test for 2-D vertical step, Re=100, ER=1.5

Table 3.6: Grid independency test for 2-D vertical backward facing step

No. of elements	Nu_{avg}
2218	0.901
7531	0.893
12027	0.894

Similarly, the grid independency test is also performed for 2-D curved backward facing step for radius of curvature of 0.007m and expansion ratio of 2.0. The curved backward facing step is discretized into 2940 elements for case 1 and then it is made finer by discretizing into 7758 and 13464 elements for case 2 and case 3 respectively. The nusselt number is determined for all the three different cases for Reynolds number 100. Figure 3.6 shows the

variation of Nusselt number with the distance from the step normalised by the step height. It is found from Fig. 3.6 that there is a significant change in the peak of nusselt number when the number of elements are increased from 2940 to 7758 but the change in results are insignificant for further increasing the number of elements in domain from 7758 to 13464. Also the average value of Nusselt number is calculated on the heated downstream wall for all the three cases. Table 3.7 shows the average nusselt number on the heated downstream wall and it is found that the change in the value of average Nusselt number is almost insignificant when the number of elements is increased from 7758 to 13464. So the optimum number of element is found to be 7758 to carry out all the numerical simulation for 2-D curved backward facing step.

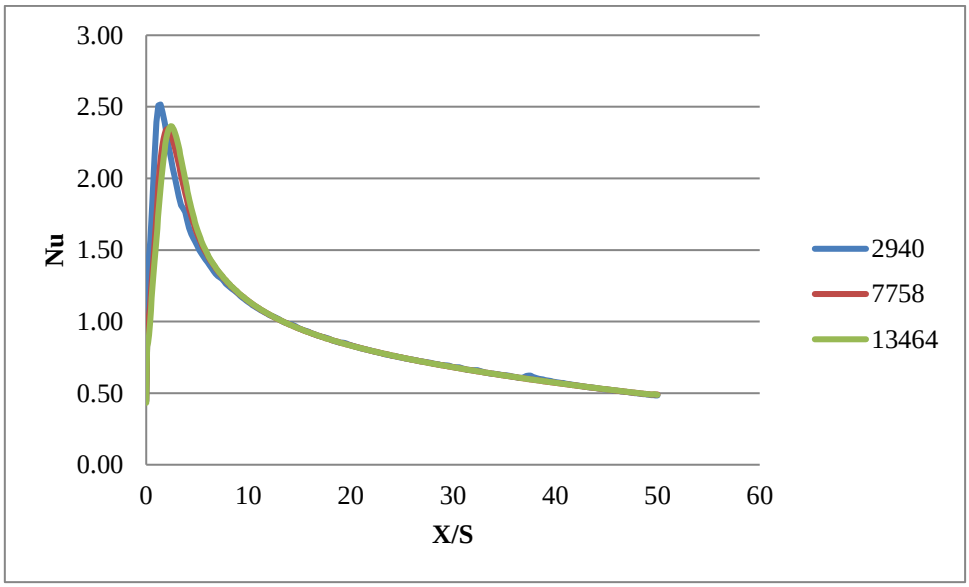

Figure 3.6: Grid Independency test for 2-D curved step, Re=100. ER=2, R=0.007m.

Table 3.7: Grid independency test for 2-D curved backward facing step

No. of elements	Nu_{avg}
2940	0.899
7758	0.892
13464	0.893

3.3 Three dimensional backward facing step

The present study deals with the investigation of three dimensional vertical and curved backward facing step. In the current study the geometrical dimensions are taken as given in

Kondoh et al. [1993]. The following section will describe the problem formulation, mesh generation, governing equations and numerical procedure used to carry out the simulation.

3.3.1 Problem description

The analysis of flow and heat transfer is also carried out over a three dimensional vertical as well as curved backward facing step for a wide range of Reynolds number covering both laminar and turbulent flow. Figure 3.7 shows a typical three dimensional vertical backward facing step and Table 3.8 shows the geometric parameters considered according to [Kondoh et al., 1993] by extruding the step in z direction. The simulation is carried out for three dimensional backward facing step having expansion ratios of 1.5 and 2.0 respectively. The upstream and downstream length of step is 0.10 m and 0.5 m respectively. The total width of the step is taken as 0.08m but due to symmetry reasons the width of the step used for simulation is kept half of it, that is L = 0.04m. The x,y and z coordinates are set to zero at the bottom of step. The bottom wall is subjected to constant temperature condition.

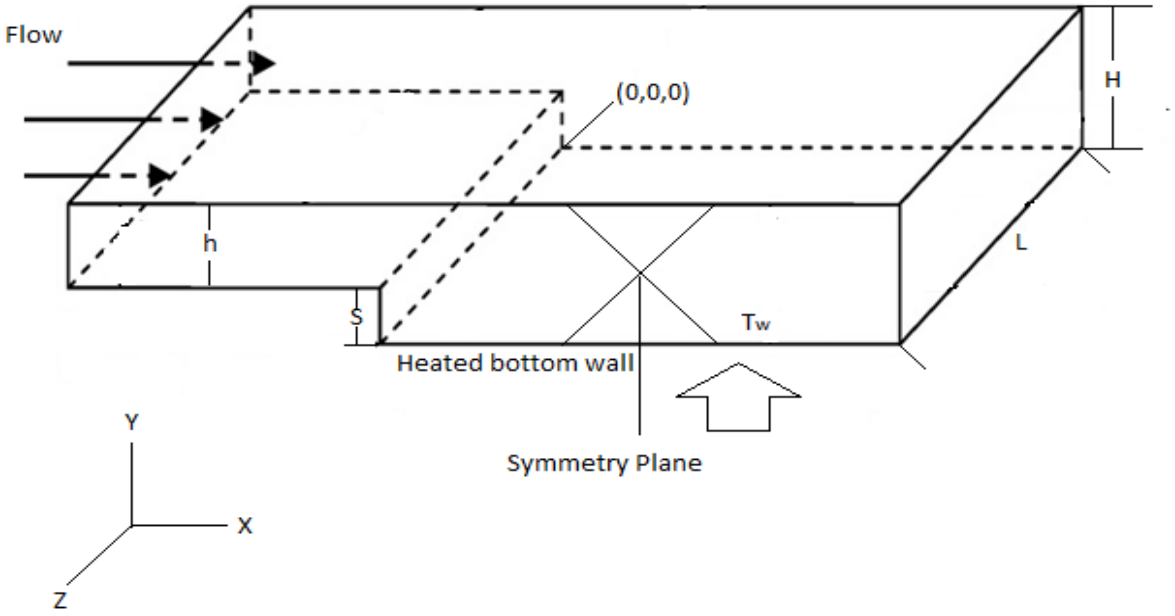

Figure 3.7: Schematic of 3-D vertical backward facing step.

Table 3.8: Geometry parameters for 3-D vertical backward facing step

Geometry Parameters	Value (m)
H	0.03
h	0.02
S	0.01
L	0.04

Similarly, the geometry for the three dimensional curved backward facing step is prepared for radii of curvature R=0.005m. The other geometric parameters are similar to vertical three dimensional backward facing step represented in Table 3.8.

3.3.2 Mesh generation

The grid is generated for the three dimensional vertical as well as curved backward facing step using quadrilateral elements in ICEM software of ANSYS Fluent. Figure 3.8 and 3.9 represents the grid generation for three dimensional vertical as well as curved backward facing step. The size of the quadrilateral element is taken as 0.0025m and 0.0022 m for vertical and curved backward facing step respectively.

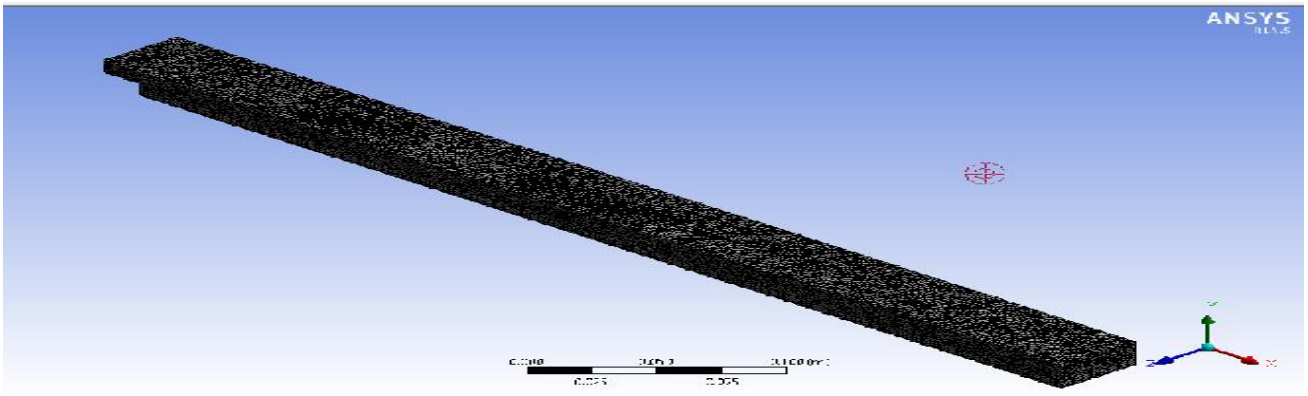

Figure 3.8: Grid generation of 3-D vertical backward facing step

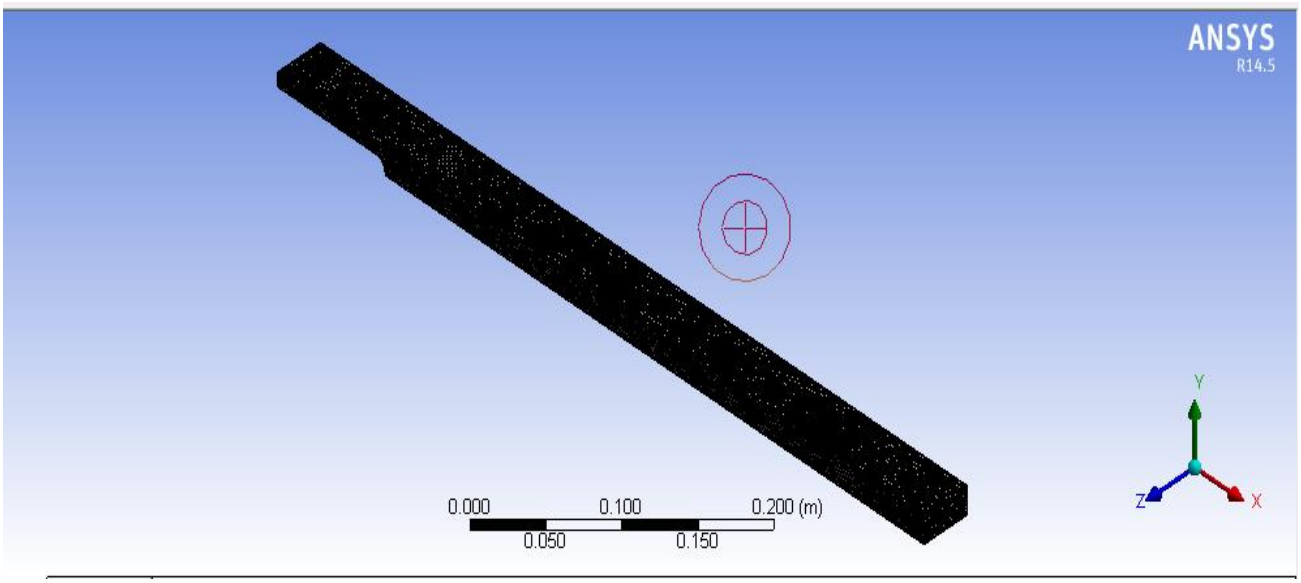

Figure 3.9: Grid generation for 3-D curved backward facing step.

3.3.3 Meshing quality parameters

The various mesh quality parameters are checked for the mesh generated in the geometry to ensure its quality. Table 3.9 and 3.10 shows the values of various mesh quality parameters for the 3-D vertical as well as curved backward facing step and it is found that all the values of mesh parameters are lying within the permissible limits.

Table 3.9: Mesh quality parameters for 3-D vertical step

Parameter	Value	Limiting value
Maximum Skewness	0.84	< 0.95
Maximum Aspect Ratio	11.83	< 35
Orthogonal Quality	0.99	Close to 1

Table 3.10: Mesh quality parameters for 3-D curved step

Parameter	Value	Desired
Maximum Skewness	0.84	< 0.95
Maximum Aspect Ratio	12.435	< 35
Orthogonal Quality	0.99	Close to 1

3.3.4 Numerical procedure

ANSYS FLUENT software is used to carry out the numerical simulation. The pressure based solver along with the viscous laminar model is chosen to solve the continuity equation, X-Y-Z momentum equation and energy equation for laminar flow and standard k-epsilon model is used to solve for turbulent flow. The SIMPLE algorithm is used for solving the Navier-Stokes equations.

3.3.5 Governing equations

The governing equations applied to this three dimensional laminar as well as turbulent flow with assumptions steady and incompressible are continuity equation, X-Y-Z momentum equations and energy equation. The equations can be written as Eq. (3.5) to (3.11).

Continuity equation

$$\frac{\partial u}{\partial x}+\frac{\partial v}{\partial y}+\frac{\partial w}{\partial z}=0 \tag{3.5}$$

Momentum equation

$$u\frac{\partial u}{\partial x}+v\frac{\partial u}{\partial y}+w\frac{\partial u}{\partial z}=-\frac{\partial p}{\rho\partial x}+\nu(\frac{\partial^2 u}{\partial x^2}+\frac{\partial^2 u}{\partial y^2}+\frac{\partial^2 u}{\partial z^2}) \tag{3.6}$$

$$u\frac{\partial v}{\partial x}+v\frac{\partial v}{\partial y}+w\frac{\partial v}{\partial z}=-\frac{\partial p}{\rho\partial y}+\nu\left(\frac{\partial^2 v}{\partial x^2}+\frac{\partial^2 v}{\partial y^2}+\frac{\partial^2 v}{\partial z^2}\right) \tag{3.7}$$

$$u\frac{\partial w}{\partial x}+v\frac{\partial w}{\partial y}+w\frac{\partial w}{\partial z}=-\frac{\partial p}{\rho\partial z}+\nu\left(\frac{\partial^2 w}{\partial x^2}+\frac{\partial^2 w}{\partial y^2}+\frac{\partial^2 w}{\partial z^2}\right) \tag{3.8}$$

Energy equation

$$u\frac{\partial T}{\partial x}+v\frac{\partial T}{\partial y}+w\frac{\partial T}{\partial z}=\alpha(\frac{\partial^2 T}{\partial x^2}+\frac{\partial^2 T}{\partial y^2}+\frac{\partial^2 T}{\partial z^2}) \tag{3.9}$$

The standard k-ε turbulence modelling scheme is employed to account the turbulence and swirling nature of flow. The transport equations which are applied to obtain the turbulent kinetic energy k and its rate of dissipation ε are given as under Eq. (3.10) to (3.11).

$$\frac{\partial}{\partial t}(\rho k)+\frac{\partial}{\partial x_i}(\rho k u_i)=\frac{\partial}{\partial x_j}\left[\left(\mu+\frac{\mu_t}{\sigma_k}\right)\frac{\partial k}{\partial x_j}\right]+G_k+G_b-\rho\varepsilon-Y_M+S_k \tag{3.10}$$

$$\frac{\partial}{\partial t}(\rho\varepsilon)+\frac{\partial}{\partial x_i}(\rho\varepsilon u_i)=\frac{\partial}{\partial x_j}\left[\left(\mu+\frac{\mu_t}{\sigma_\varepsilon}\right)\frac{\partial \varepsilon}{\partial x_j}\right]+C_{1\varepsilon}\frac{\varepsilon}{k}(G_k+C_{3\varepsilon}G_b)-C_{2\varepsilon}\rho\frac{\varepsilon^2}{k}+S_\varepsilon \tag{3.11}$$

Where G_k represents the generation of turbulent kinetic energy due to mean velocity gradients, G_b stands for generation of turbulent kinetic energy due to buoyancy. Y_M represents the contribution of the fluctuating dilatation in compressible turbulence to the overall dissipation rate. $C_{1\varepsilon}$, $C_{2\varepsilon}$, $C_{3\varepsilon}$ are constants and σ_k, σ_ε are the turbulent Prandtl numbers for k and ε respectively. S_k and S_ε are user defined source terms.

The turbulent viscosity (μ_t) is computed with the help of k and ε as under:

$$\mu_t = \rho C_\mu \frac{k^2}{\varepsilon}$$

Where C_μ is a constant.

Table 3.11 shows the value of the model constants used in the k- ε model.

Table 3.11: Model constants

Constant	$C_{1\varepsilon}$	$C_{2\varepsilon}$	σ_ε	σ_k	C_μ
Value	1.44	1.92	1.3	1	0.09

$C_{3\varepsilon}$ can be calculated as

$$C_{3\varepsilon} = \tanh\left|\frac{\mathrm{v}}{\mathrm{u}}\right|$$

Where v refers to the velocity of flow along the direction of gravity and u refers to the velocity of flow in the direction normal to the direction of gravity. $C_{3\varepsilon}$ = 1 for buoyant shear layers for which the direction of the main flow lies along the direction of gravity and $C_{3\varepsilon}$ = 0 for buoyant shear layers for which the direction of the main flow lies in the direction normal to the direction of gravity.

3.3.6 Boundary conditions

The boundary conditions applied for the solutions are as follows:

- At inlet: u = u_{in} and v=0, w=0, T_f =300K
- At outlet: Gauge pressure=0

- At walls: walls are kept stationary and with no slip condition. The heated wall is maintained at constant temperature of 310K while others are insulated.

3.3.7 Convergence criteria

Table 3.12 shows the convergence criteria specified for continuity equation, x-velocity, y-velocity, z-velocity, turbulent kinetic energy, turbulent dissipation rate, turbulent viscosity and energy equation in the numerical simulation.

Table 3.12: Convergence criteria for 3-D turbulent flow

Parameter	**Convergence Criteria**
Continuity	0.001
X-Veocity	0.001
Y-Velocity	0.001
Z-Velocity	0.001
Energy	1e-06
k	0.001
Epsilon	0.001

3.3.8 Under relaxation factors

Table 3.13 shows the under relaxation factors used for different parameters involved in the numerical solution of flow and heat transfer over the backward facing step.

Table 3.13: Under relaxation factors for 3-D turbulent flow

Parameter	Value
Pressure	0.3
Density	1
Body forces	1
Momentum	0.7
Turbulent kinetic energy	0.8
Turbulent dissipation rate	0.8
Turbulent viscosity	1
Energy	1

3.3.9 Grid independency test

The grid independency test is performed to make the results independent of the grid size after a particular number of elements. The present study considers three different cases for the grid independency test. The 3-D vertical backward facing step with expansion ratio 1.5 is discretized into 276585 elements for case 1 and then it is made finer by discretizing into 385365 and 565385 elements for case 2 and case 3 respectively. The model is simulated using governing equation represented in Eq. (3.5) to (3.11) along with the boundary conditions represented in section 3.3.6. The properties of air, convergence criteria and under relaxation factors represented in Table 3.3 and Table (3.12) to (3.13) are also used for the numerical simulation for all the three different cases. The nusselt number is determined for all the three different cases for Reynolds number 100. Table 3.14 shows the value of average Nusselt number on the heated downstream wall. It is found from the Table 3.14 that there is a significant change in the average value of nusselt number when the number of elements are increased from 276585 to 385365 but the change in results are insignificant for further increasing the number of elements in domain from 385365 to 565385. So the optimum number of element is found to be 385365 which is used further for numerical simulation.

Table 3.14: Grid independency test for 3-D vertical backward facing step

No. of elements	Nu_{avg}
276585	0.62
385365	0.64
565385	0.65

Similarly, the grid independency test is also performed for 3-D curved backward facing step for radius of curvature of 0.005m and expansion ratio of 2.0. The curved backward facing step with is discretized into 285848 elements for case 1 and then it is made finer by discretizing into 368343 and 495156 elements for case 2 and case 3 respectively. The nusselt number is determined for all the three different cases for Reynolds number 100. Table 3.15 shows the average value of Nusselt number along the heated downstream wall. It is found from Table 3.15 that there is a small change in the average value of nusselt number when the number of elements are increased from 285848 to 368343 but the change in results are almost none for further increasing the number of elements in domain from 368343 to 495156. So the

optimum number of element is found to be 495156 to carry out all the numerical simulation for 3-D curved backward facing step.

Table 3.15: Grid independency test for 3-D curved backward facing step

No. of elements	Nu_{avg}
285848	0.582
368343	0.599
495156	0.593

3.3.10 Concluding remarks

The present chapter model the geometry of two dimensional and three dimensional vertical as well as curved backward facing step. The grid is generated and mesh quality parameters are checked and it is found that the mesh quality parameters are within the permissible limit. The grid independency test is carried out to determine the optimum of number of elements required for simulation. The optimum number of elements selected for 2-D vertical and curved backward facing step is 7531 and 7758 respectively. The optimum number of elements selected for 3-D vertical and curved facing step is 385365 and 368343 respectively.

Chapter 4

Results and Discussion

4.1 Introductory comment

The present chapter analyses the various results obtained from the simulation of two and three dimensional vertical as well as curved backward facing step. The reattachment length and Nusselt number are calculated for a wide range of Reynolds number covering both laminar and turbulent flow. Also the reattachment length and Nusselt number are calculated for various expansion ratios. The results are validated with published literature. The flow characteristics are obtained for vertical backward facing step as well as for the curved backward facing step incorporating laminar as well as turbulent flow. The results obtained from the curved backward facing step are compared with the vertical backward facing step.

4.2 Two dimensional vertical backward facing step

The study conducted for the laminar and turbulent flow over a 2-D backward facing step yielded many results which enable a deep insight into the flow behaviour and rate of heat transfer during the flow. The governing Eq. (3.1) to (3.4) and (3.10) to (3.11) along with boundary conditions (3.2.6) are used for the simulation of the model. The results of numerical simulation are validated with Kondoh et al. [1993].

4.2.1 Model validation

An attempt is made to validate the results of the present study with Kondoh et al. [1993]. The model is simulated using governing equation represented in Eq. (3.1) to (3.4) along with the boundary conditions represented in section 3.2.6. The properties of air, convergence criteria and under relaxation factors represented in Table (3.3) to (3.5) are also used for the numerical simulation. The Nusselt number is determined at the boundary wall of heated surface. Figure 4.1 shows the variation of Nusselt number with the distance from the step normalised by the step height for Re = 100 and expansion ratio of 1.5.

The results obtained in the current study are compared with the results obtained by Kondoh et al. [1993] numerically and found in good agreement with Kondoh et al. [1993].

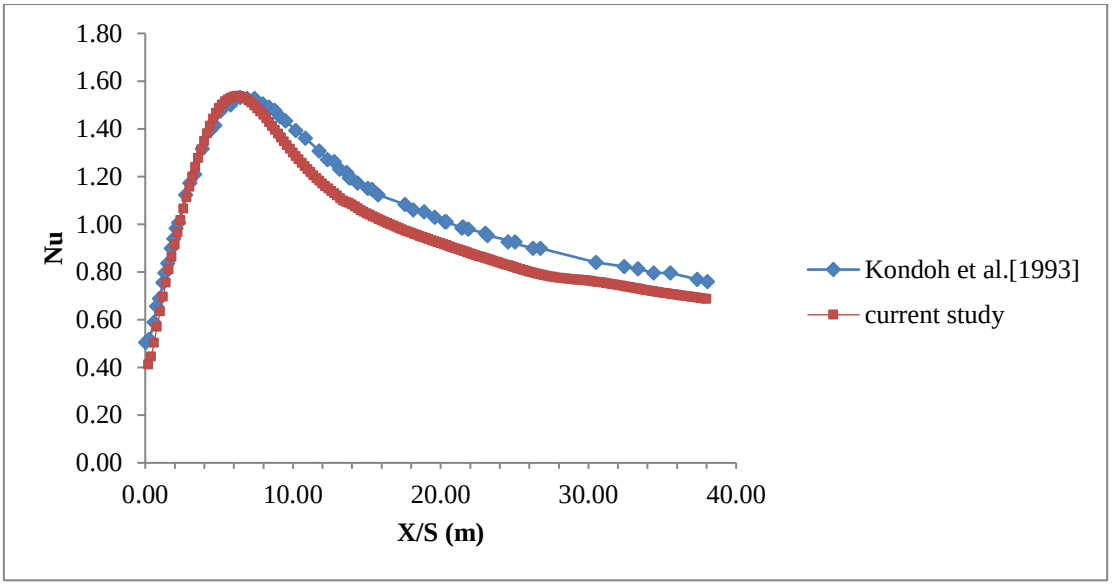

Figure 4.1: Comparison of Nusselt number for 2-D vertical step, Re=100, ER=1.5.

4.2.2 Effect of Reynolds number

The effect of Reynolds number has been studied on Nusselt number for laminar as well as turbulent flow. Reynolds number has been varied through wide range which covers both laminar and turbulent regime. Eq. (4.1) represents the Reynolds number used in the present study.

$$\mathrm{Re} = \frac{ud}{\nu} \tag{4.1}$$

Where u is the inlet velocity, d is hydraulic diameter which is equal to step height and ν is kinematic viscosity of fluid.

Figure 4.2 shows the variation of the Nusselt number with the distance from the step normalised by the step height for various Reynolds ranging from 50-200 which covers laminar flow. The peak of Nusselt number shifts towards the right for higher Reynolds number because the recirculation region along with reattachment point is drifted away from the step for higher Reynolds number. The peak of Nusselt number is found near the reattachment point as the recirculation region formed will throw the heated fluid from the wall surface to the upper fluid layers and consequently the heat transfer is enhanced steeply. This entrainment of the hot fluid from the bottom to the top fluid layers also results in the contraction of thermal boundary layer.

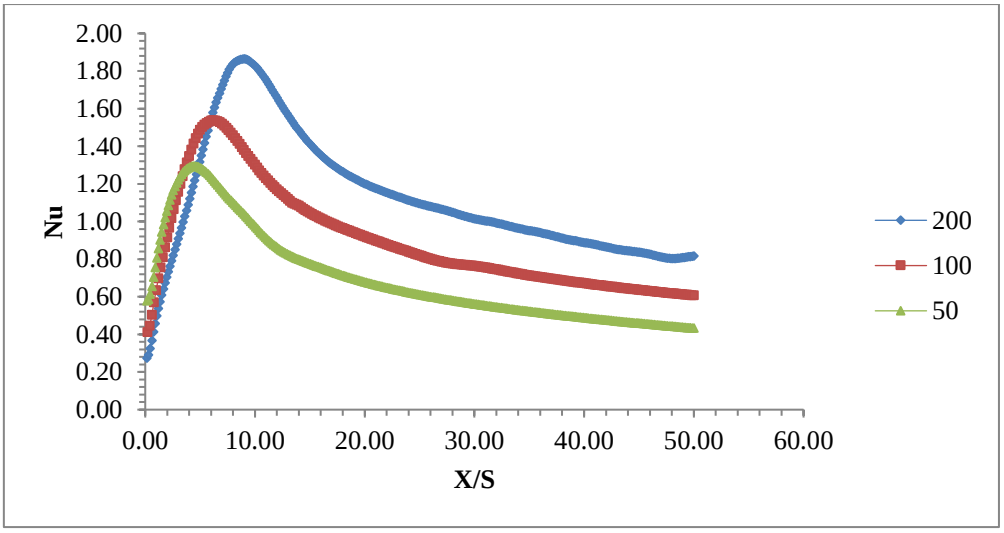

Figure 4.2: Variation of Nu with X/S for laminar flow, ER=1.5.

Figure 4.3 shows the variation of the Nusselt number with the distance from the step normalised by the step height for different Reynolds number having the expansion ratio 1.5. The Reynolds number considered are ranging from 3000-9000 which covers the region of transition to turbulent flow. It is found from Fig that the peak of Nusselt number is found to increase for higher Reynolds number which is in similar to the laminar flow but the location of the peak Nusselt number does not change significantly for turbulent flow as the change in the zone of recirculation region during turbulent flow is almost insignificant. The average value of the Nusselt number is found out. Figure 4.4 shows the variation of average Nusselt number with the different Reynolds number covering both the laminar and turbulent flow. The average Nusselt number is found to increase with increasing the Reynolds number.

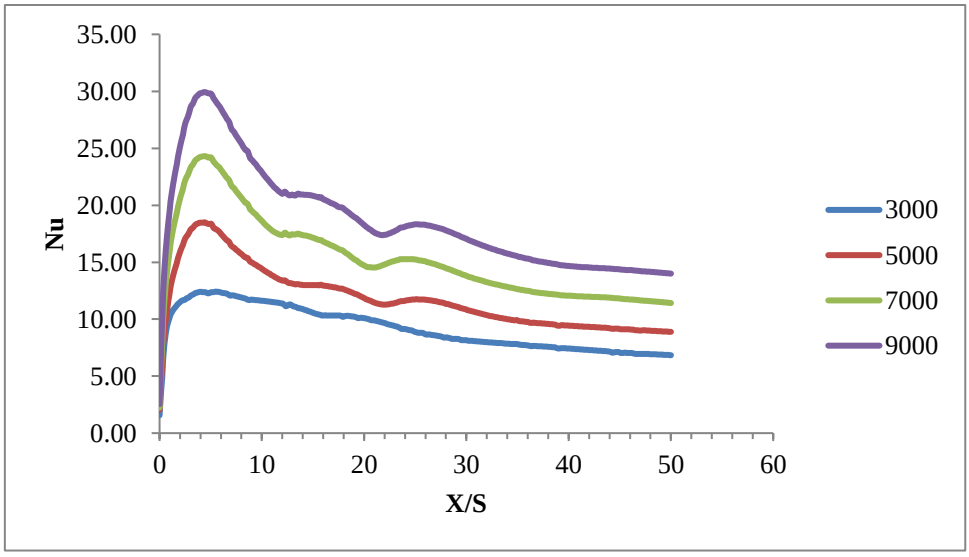

Figure 4.3: Variation of Nu with X/S for turbulent flow, ER=1.5.

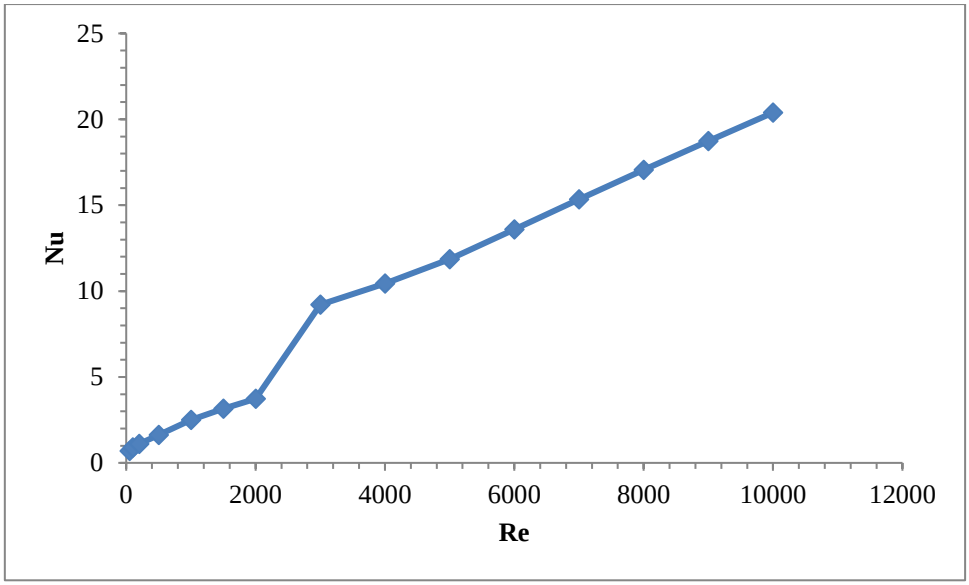

Figure 4.4: Variation of Nu with Re for 2-D vertical step, ER=1.5.

The present study also determined the reattachment length for the flow over the backward facing step and it is found that the reattachment length is a function of Reynolds number. Figure 4.5 shows the variation of reattachment length with different Reynolds number covering the laminar as well as turbulent flow for the backward facing step having expansion ratio 1.5. The reattachment length is found to be increased with increase in Reynolds number upto 500 and then the reattachment length decreased upto the Reynolds number 2500. The variation of reattachment length is found insignificant for further increasing in The Reynolds number. The increasing reattachment length with Reynolds number upto 500 can be characterised as laminar flow where as the decreasing the reattachment length with Reynolds number from 500-2500 can be characterised as the transition flow and the constant reattachment length for Reynolds number beyond 2500 can be characterised as the turbulent flow. The similar trend of reattachment with Reynolds number has been reported in the literature. The present study is made by heating the bottom plate of backward facing step and the trend of the variation of reattachment length with Reynolds number is also similar reported by [Armaly et al., 1983] and [Ratha and Sarkar, 2015] for the flow over a backward facing step without any heat transfer study. Only the value of Reynolds number in the present study where the flow regime changes, are different from the [Armaly et al., 1983] and [Ratha and Sarkar, 2015]. Table 4.1 shows the flow regime obtained at various Reynolds number in the present study and its comparison with the other published literature.

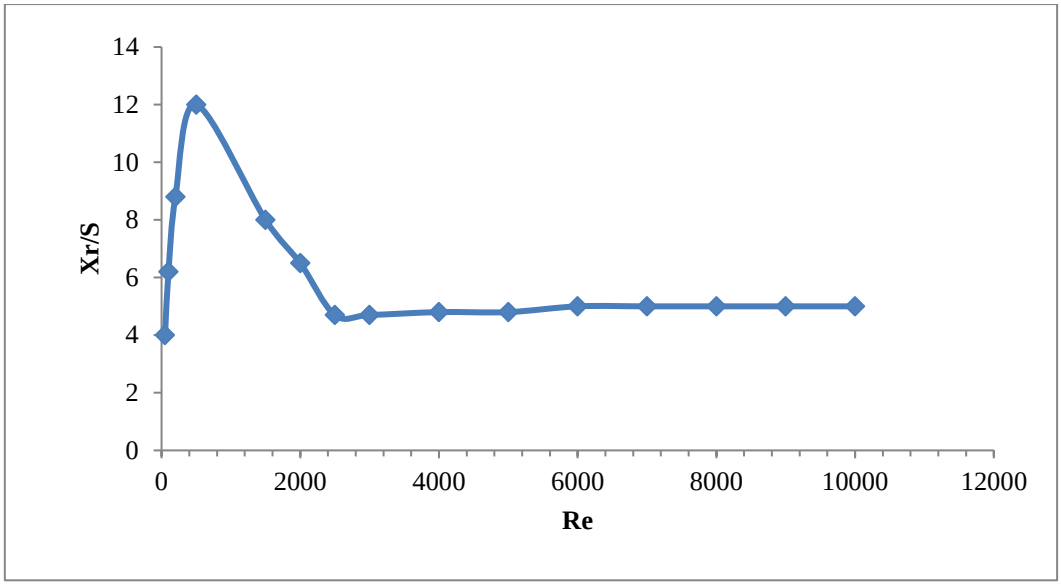

Figure 4.5: Variation of reattachment length with Re for 2-D vertical step, at ER=1.5.

Table 4.1: Comparison of flow regimes occur in present study with the literature available.

Type of flow	Armaly et al. (1983) (without heat transfer)	Ratha and Sarkar (2015) (without heat transfer)	Present study (with heat transfer)
Laminar	Upto Reynolds no 1200	Upto Reynolds no 900	Upto Reynolds no 500
Transion	Reynold no 1200-6600	Reynolds no 900-5600	Reynolds no 500-2500
Turbulent	Reynold no > 6600	Reynold no > 5600	Reynold no > 2500

4.2.3 Effect of expansion ratio

The expansion ratio of a backward facing step can be changed by two ways, one is by varying the inlet channel height namely case 1 and another is by varying the step height namely case 2. Figure (4.6) to (4.9) belongs to the case 1 and Fig. (4.10) to (4.11) belongs to case 2. Figure 4.6 shows the effect of expansion ratio on the value of Nusselt number with a distance from the step normalised by the step height. From the Fig. 4.6 it is clear that the increase in expansion ratio increases the Nusselt number and consequently the rate of heat transfer. The increase in Nusselt number results as the increase in expansion ratio leads to decrease in the inlet channel height for constant step height. This basically increases the intensity of flow for same Reynolds number and enhances the heat transfer.

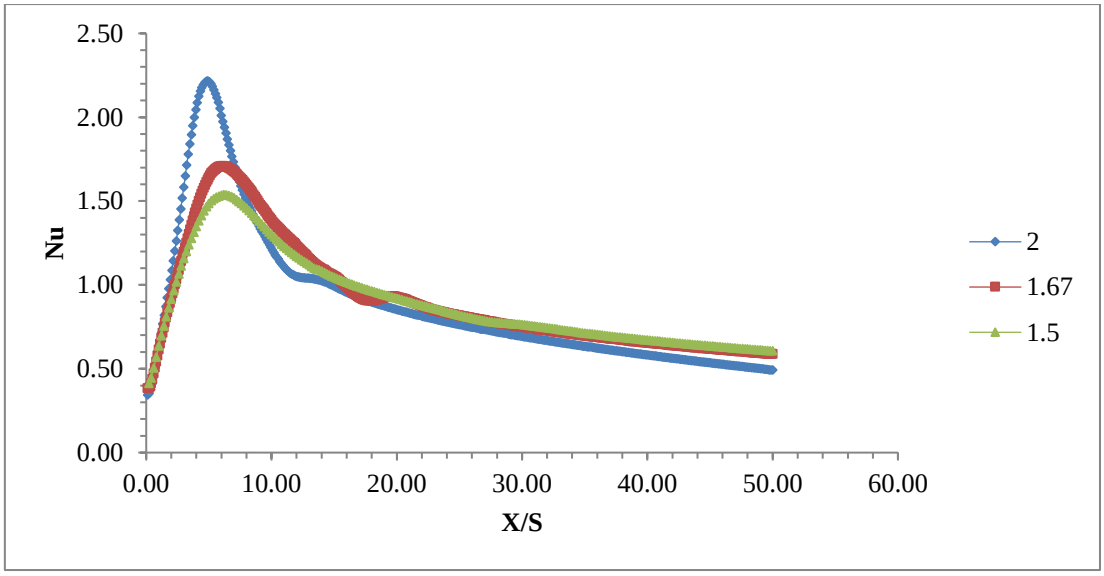

Figure 4.6: Variation of Nusselt number with X/S, for ER=1.5,1.67,2.

Figure 4.7 shows the effect of expansion ratio on the Nusselt number for different Reynolds number covering laminar as well as turbulent flow. It is concluded from the graph that Nusselt number increases with increase in Reynolds number for different expansion ratio. The magnitude of Nusselt number is coinciding for different expansion ratio upto transition zone and there after the magnitude of Nusselt number lies below for the higher expansion ratio.

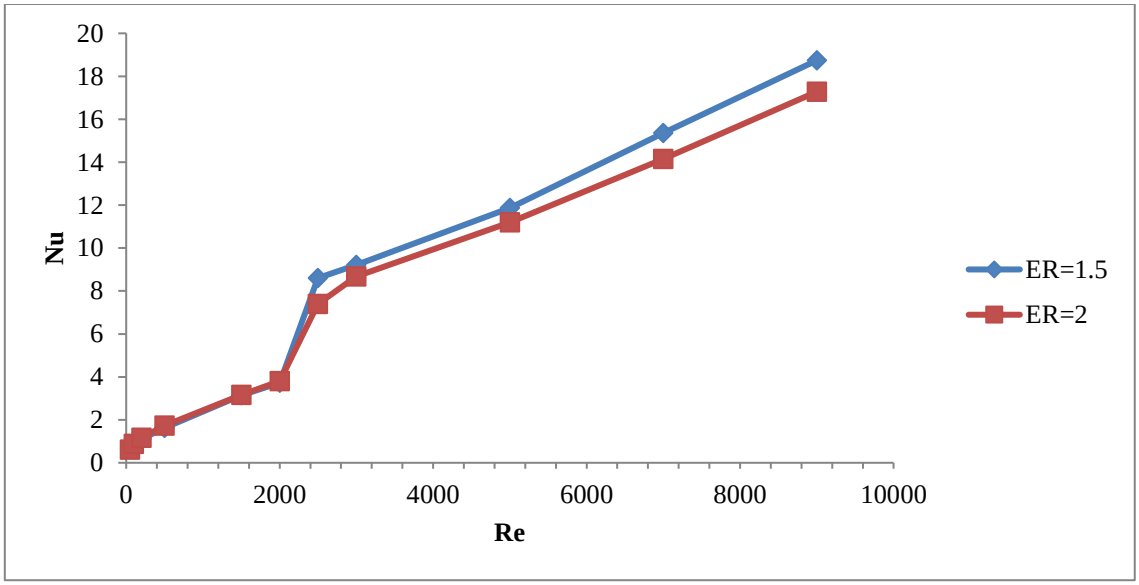

Figure 4.7: Variation of Nu with different ER for laminar and turbulent flow.

Figure 4.8 shows the variation of reattachment length with expansion ratio for the constant value of Reynolds number 100. The expansion ratios used for carrying out the present study

are 1.5,1.67 and 2. It is found that the reattachment length decreases with increase in expansion ratio.

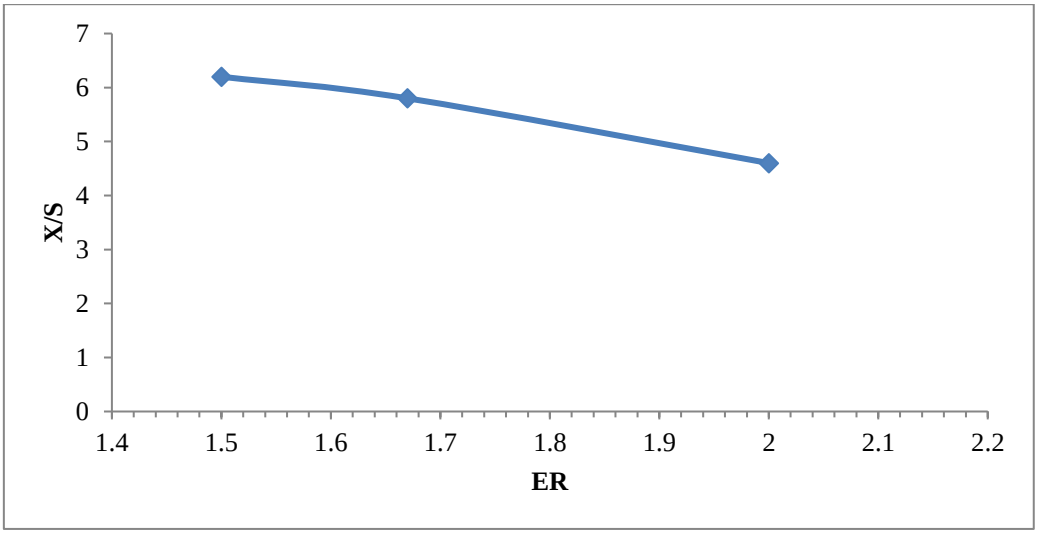

Figure 4.8: Variation of reattachment length with ER at Re=100.

Figure 4.9 shows the variation of the reattachment length with different Reynolds number covering laminar as well as turbulent flow for different expansion ratios 1.5 and 2. The reattachment length is found increasing with Reynolds number in the laminar region and then decreases in the transition region and thereafter remains almost steady in the turbulent region for all expansion ratios. The magnitude of the reattachment length for higher expansion ratio is found to be less during the laminar and transition flow and the magnitude of the reattachment length is found to be more in the turbulent regime for higher expansion ratio.

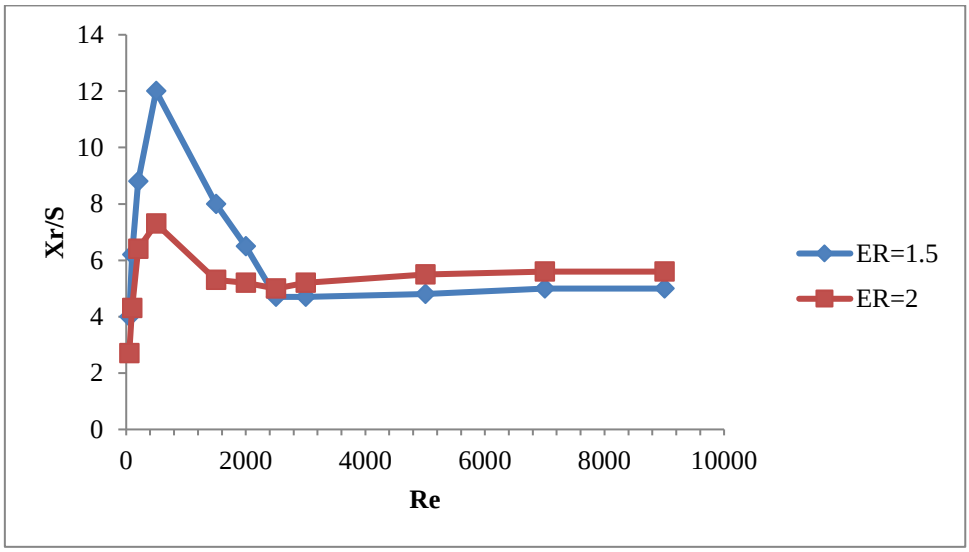

Figure 4.9: Variation of reattachment length with different ER for laminar and turbulent flow.

Figure 4.10 shows the effect of expansion ratio on the Nusselt number for different Reynolds number covering laminar as well as turbulent flow. It is concluded from the graph that Nusselt number increases with increase in Reynolds number for different expansion ratio. The magnitude of Nusselt number is coinciding for different expansion ratio upto transition zone and there after the magnitude of Nusselt number lies below for the higher expansion ratio.

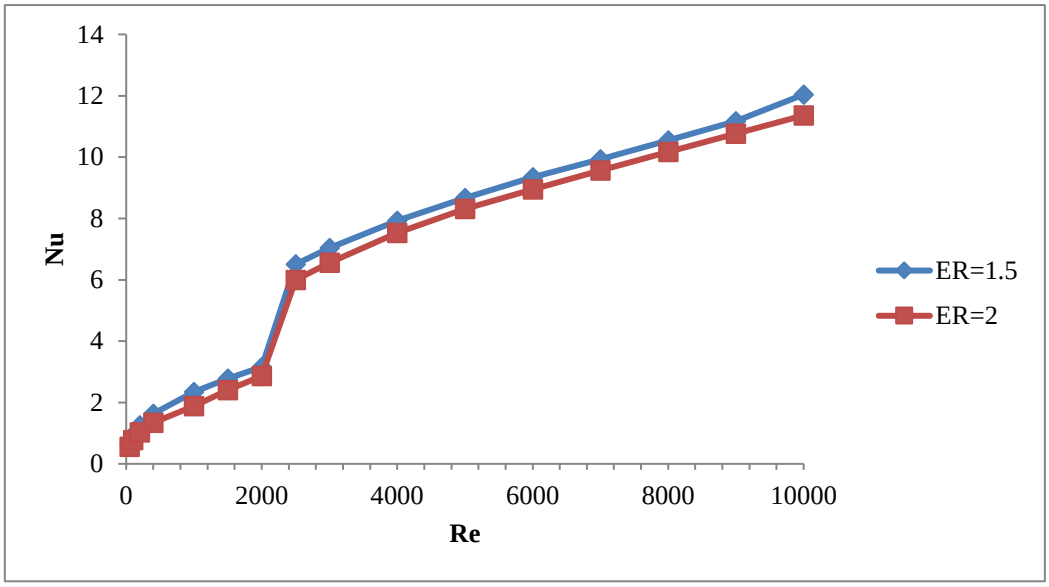

Figure 4.10 Variation of Nu with different ER for laminar and turbulent flow.

Figure 4.11 shows the variation of the reattachment length with different Reynolds number covering laminar as well as turbulent flow for different expansion ratios 1.5 and 2. The reattachment length is found increasing with Reynolds number in the laminar region and then decreases in the transition region and thereafter remains almost steady in the turbulent region for all expansion ratios. The magnitude of the reattachment length for higher expansion ratio is found to be more during the laminar, transition and turbulent flow.

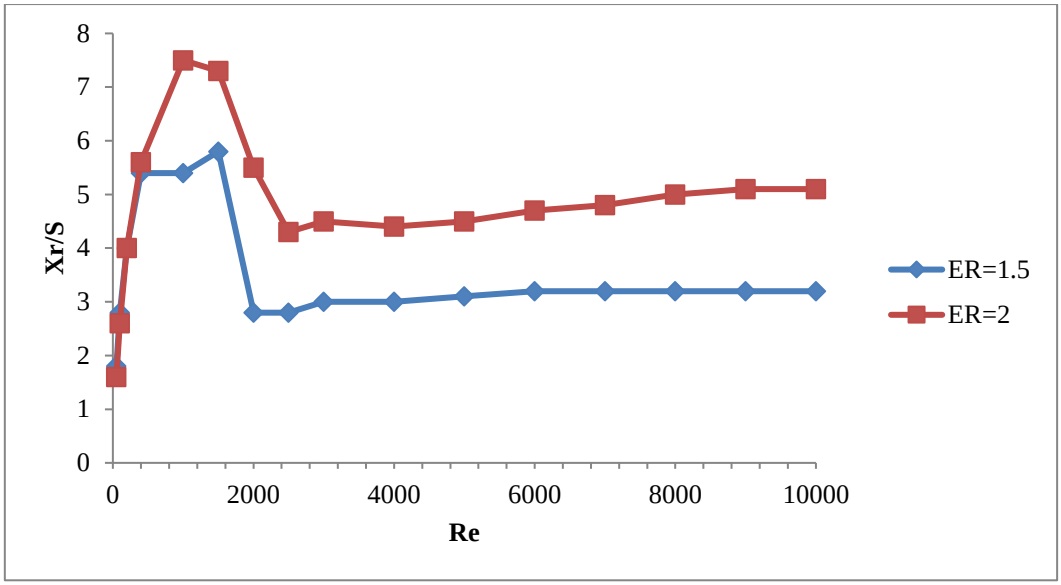

Figure 4.11: Variation of reattachment length with different ER for laminar and turbulent flow.

4.2.4 Velocity profile

The variation of both horizontal and vertical component of velocity in *x-y* plane is also studied for vertical backward facing step. Figure (4.12) to (4.14) shows the vertical variation of horizontal component of velocity at different longitudinal section downstream of the step for the Reynolds number ranging from 50-200 for ER=1.5. It is found that the recirculation region is existing up to 3.0 m, 5.4m, 8.2m from the step for Reynolds number 50, 100 and 200 respectively.

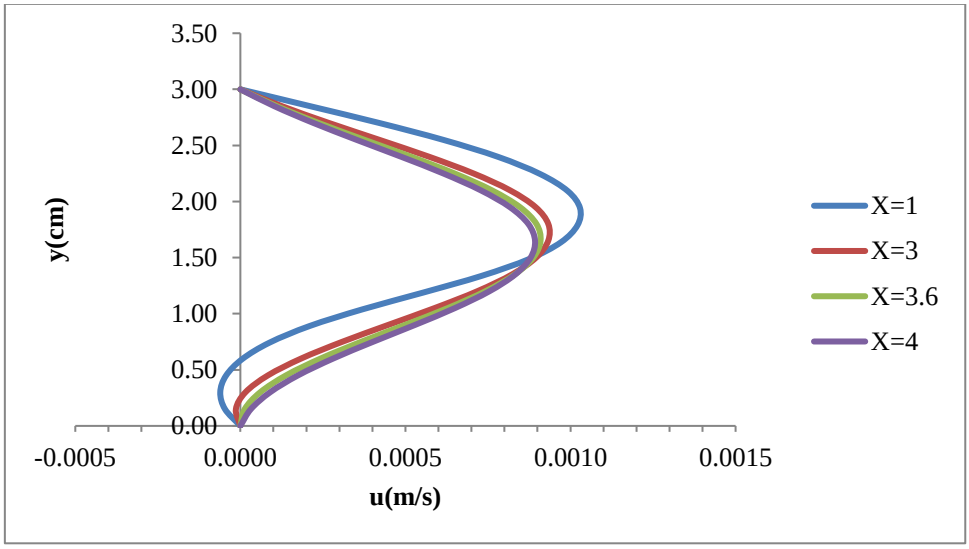

Figure 4.12: velocity profile for x-component, Re=50, ER=1.5.

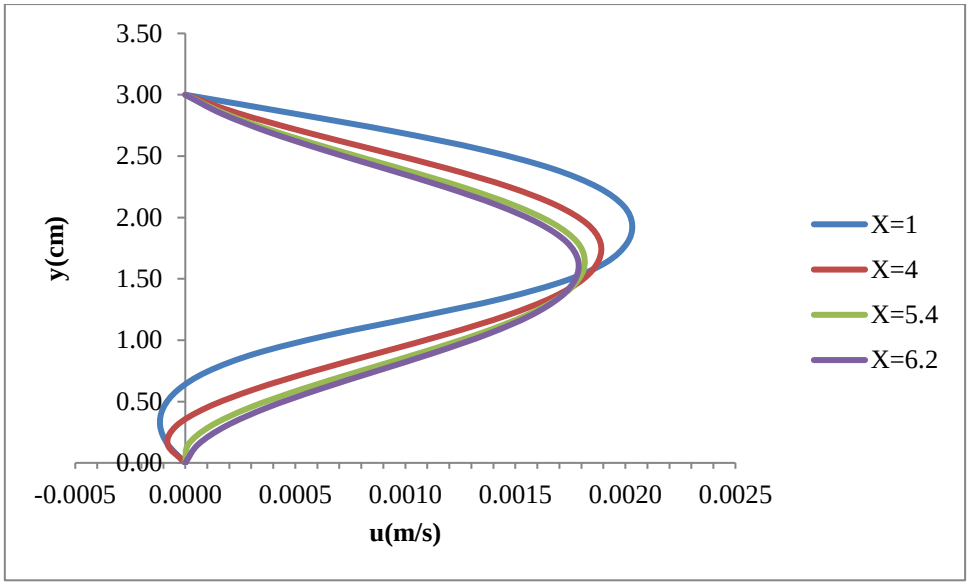

Figure 4.13: Velocity profile for x-component, Re=100, ER=1.5.

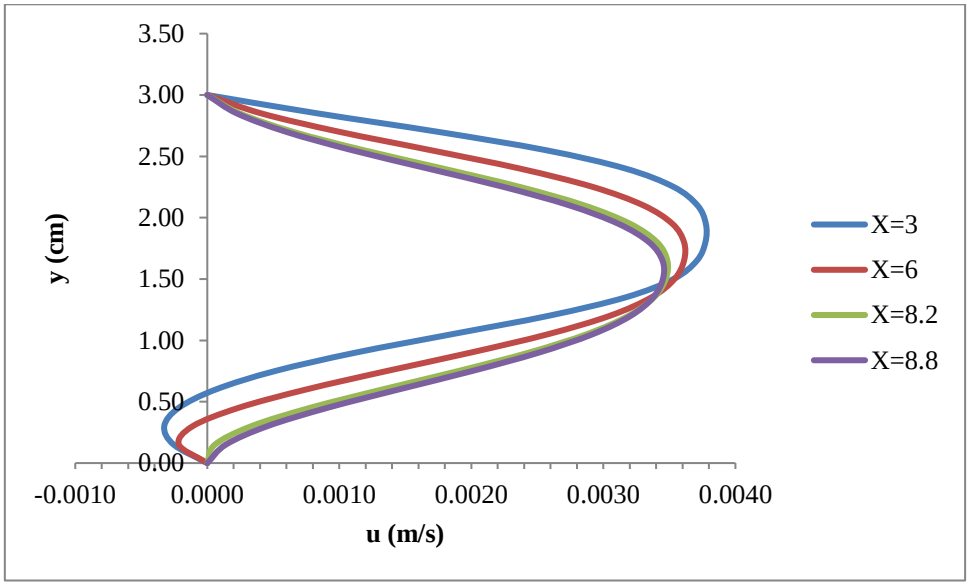

Figure 4.14: Velocity profile for x-component, Re=200, ER=1.5.

Figure 4.15 shows the variation of y-component of the velocity with the distance from the step normalised by the step height for different values of Reynolds number covering the laminar flow. The velocity in y-direction first increases just after the step due to formation of recirculation region. Then the y-velocity starts decreasing and takes the minimum value near the reattachment point. The vertical component of velocity starts increasing beyond the reattachment point till the attainment of fully developed flow.

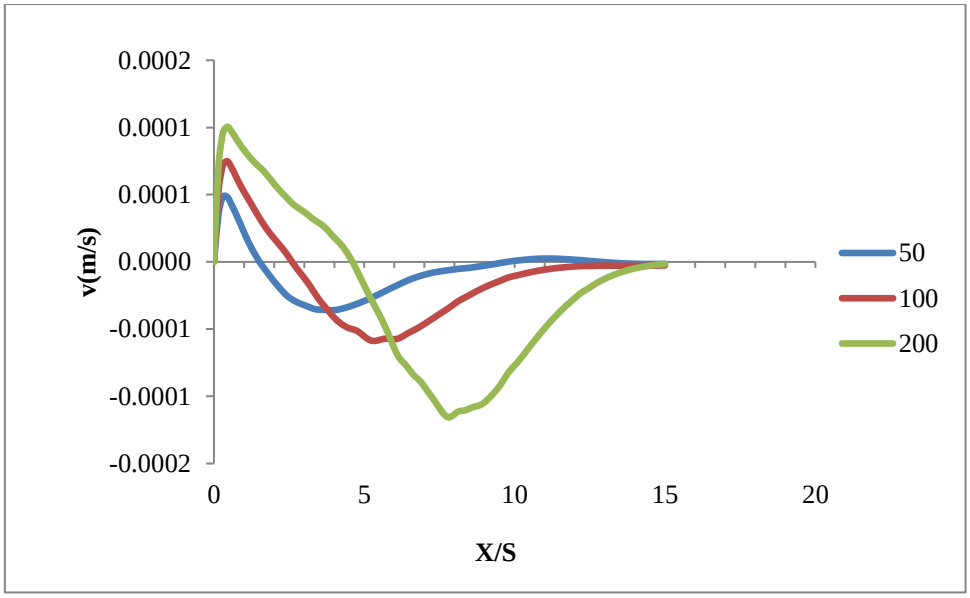

Figure 4.15: Velocity profile for y-component, Re=50,100,200, ER=1.5, Y/S=0.01.

4.2.5 Skin friction coefficient

Figure 4.16 shows the variation of skin friction coefficient with the distance from the step normalised by the step height different Reynolds number covering lamianr flow. The decrease in skin friction coefficient is noted with increase in Reynolds number. The skin friction coefficient is found to be less in recirculation region and after recirculation region it increases and then becomes almost constant.

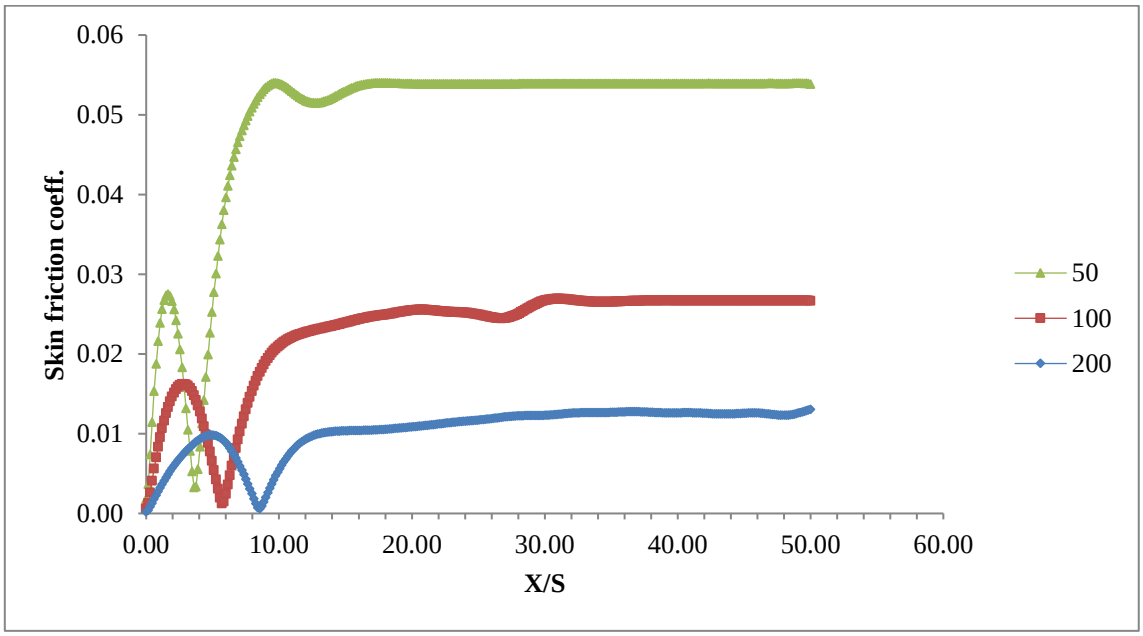

Figure 4.16: Comparison of skin friction coefficient for Re=50,100,200 with ER=1.5

4.2.6 Wall shear stress

Figure 4.17 shows the variation of shear stress with a distance from the step normalised by the step height different Reynolds number covering lamianr flow. The shear stress is found to increase first and then decreases and becomes zero at the reattachment point. After that the shear stress again starts increasing and becomes constant when flow approaches fully developed channel flow.

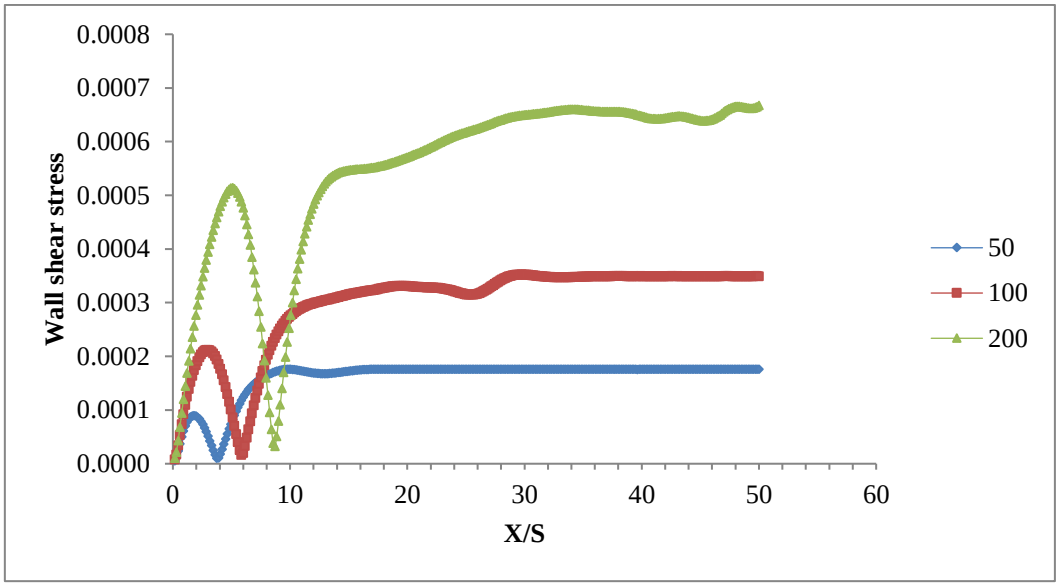

Figure 4.17: Wall shear stress variation for different Re, ER=1.5.

4.3 Two dimensional curved backward facing step

The present study also carried out to analyse the flow and heat transfer characteristics for the curved backward facing step. The results are obtained for different values of radius of curvature at different Reynolds number and expansion ratios. The variation for reattachment length and Nusselt number incorporating both laminar and turbulent flow has been studied in the present numerical study.

4.3.1 Effect on Nusselt number

Figure 4.18 shows the variation of average Nusselt number with the Reynolds number covering laminar as well as turbulent flow for expansion ratio of 2 and radius of curvature 0.007m. The average value of Nusselt number is calculated on the downstream heated wall. The average value of Nusselt number is found to increase with the Reynolds number. The

sudden increase in the average value of Nusselt number can be observed for Reynolds number 2500 as fluid regime becomes turbulent.

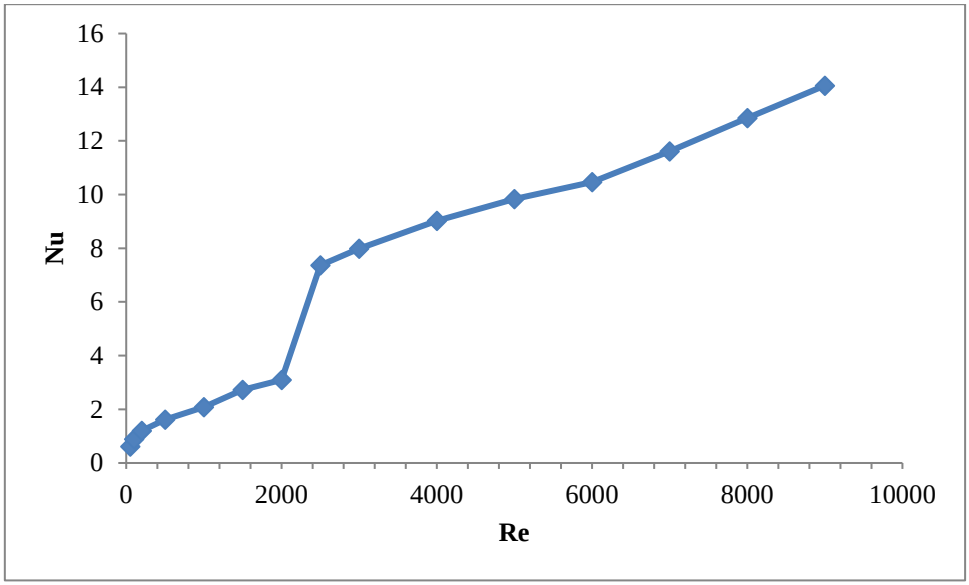

Figure 4.18: Variation of Nu with Re for 2-D curved step, ER=2, R=0.007m.

4.3.2 Effect on reattachment length

Figure 4.19 shows the variation of reattachment length with the Reynolds number for expansion ratio of 2 and radius of curvature 0.007m. The reattachment length is found to increase in the laminar range up to Reynolds number 1000 and it starts decreasing in the transition phase for Reynolds number 1000-2500. The reattachment length is observed to remain almost constant throughout the turbulent flow at Reynolds number 2500 onwards.

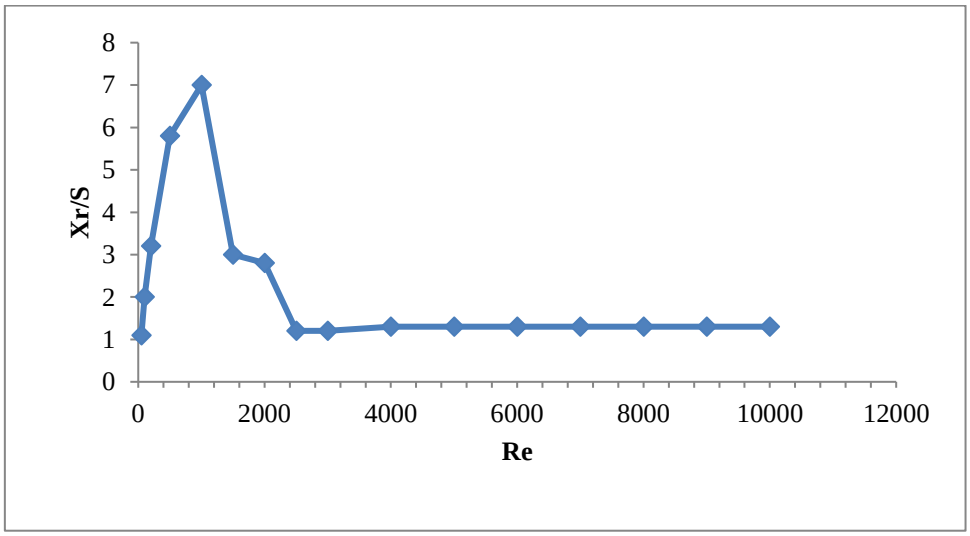

Figure 4.19: Variation of reattachment length with Re for 2-D curved step, ER=2, R=0.007m.

4.3.3 Effect of expansion ratio

The expansion ratio of a backward facing step can be changed by two different ways; one is by varying the inlet channel height namely case 1 and another is by varying the step height namely case 2. Figure (4.20) to (4.21) belongs to case 1 and Fig. (4.22) to (4.23) belongs to case 2. Figure 4.20 shows the effect of expansion ratio on the Nusselt number for different Reynolds number covering laminar as well as turbulent flow. It is concluded from the graph that Nusselt number increases with increase in Reynolds number for different expansion ratio. The magnitude of Nusselt number is coinciding for different expansion ratio up to transition zone and there after the magnitude of Nusselt number lies below for the higher expansion ratio.

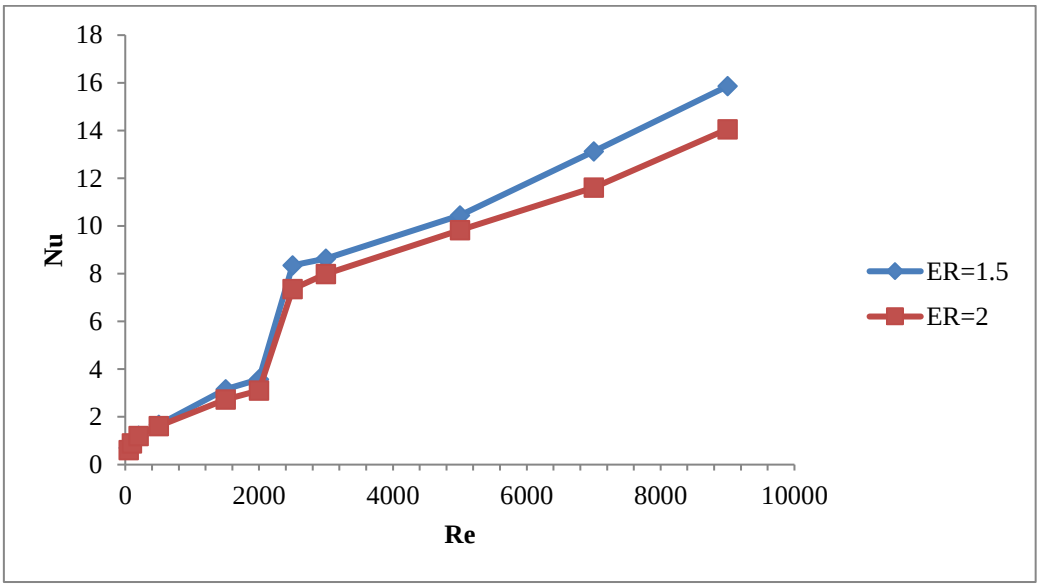

Figure 4.20: Effect of expansion ratio on Nu for different Re, R=0.007m.

Figure 4.21 shows the variation of the reattachment length with different Reynolds number covering laminar as well as turbulent flow for different expansion ratios 1.5 and 2. The reattachment length is found increasing with Reynolds number in the laminar region and then decreases in the transition region and thereafter remains almost steady in the turbulent region for all expansion ratios. The magnitude of the reattachment length for higher expansion ratio is found to be less during the laminar and transition flow and the magnitude of the reattachment length is found to be more in the turbulent regime for higher expansion ratio.

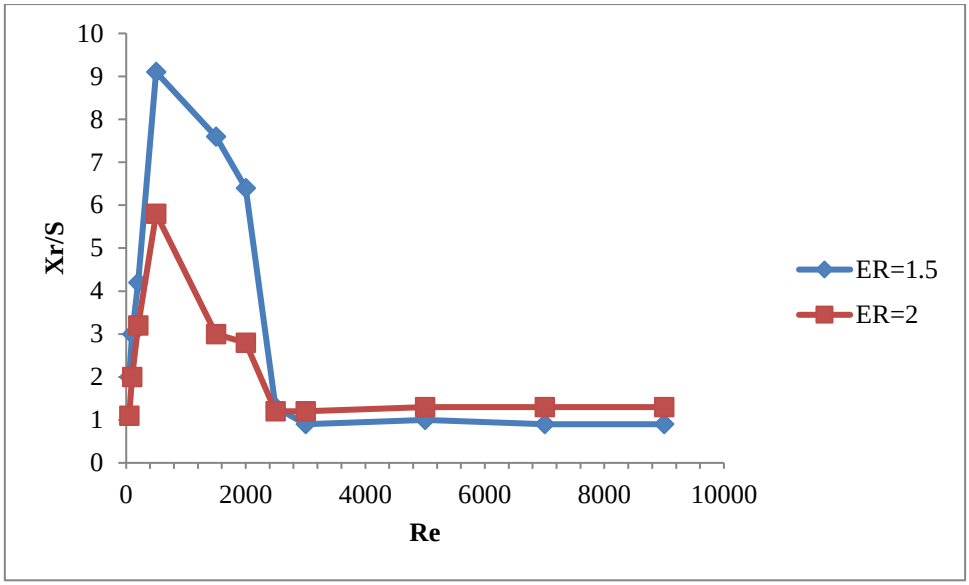

Figure 4.21: Effect of expansion ratio on Xr/S for different Re, R=0.007m.

Figure 4.22 shows the effect of expansion ratio on the Nusselt number for different Reynolds number covering laminar as well as turbulent flow. It is concluded from the graph that Nusselt number increases with increase in Reynolds number for different expansion ratio. The magnitude of Nusselt number is coinciding for different expansion ratio up to transition zone and there after the magnitude of Nusselt number lies below for the higher expansion ratio.

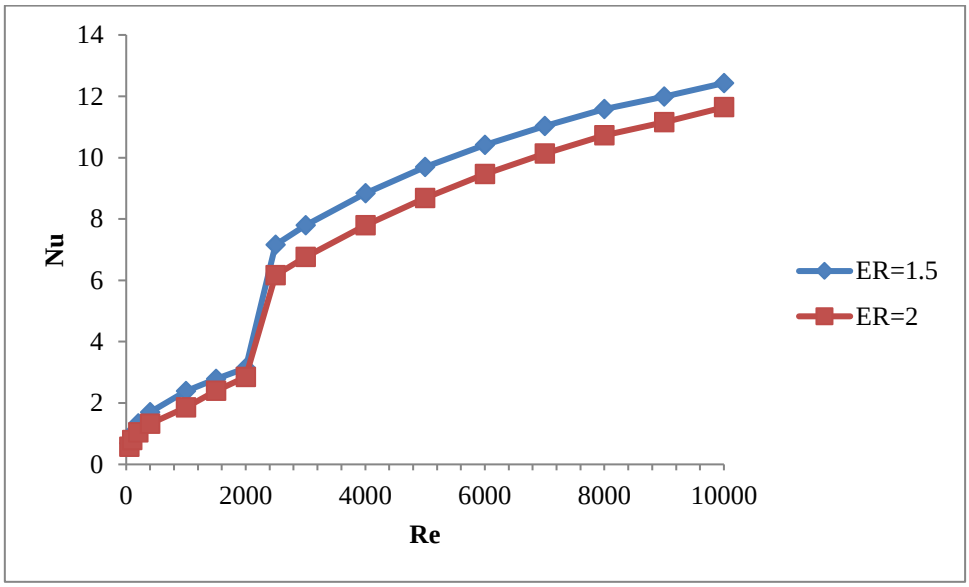

Figure 4.22: Effect of expansion ratio on Nu for different Re, R=0.005m.

Figure 4.23 shows the variation of the reattachment length with different Reynolds number covering laminar as well as turbulent flow for different expansion ratios 1.5 and 2. The reattachment length is found increasing with Reynolds number in the laminar region and then decreases in the transition region and thereafter remains almost steady in the turbulent region for all expansion ratios. The magnitude of the reattachment length for higher expansion ratio is found to be more during the laminar, transition and turbulent flow.

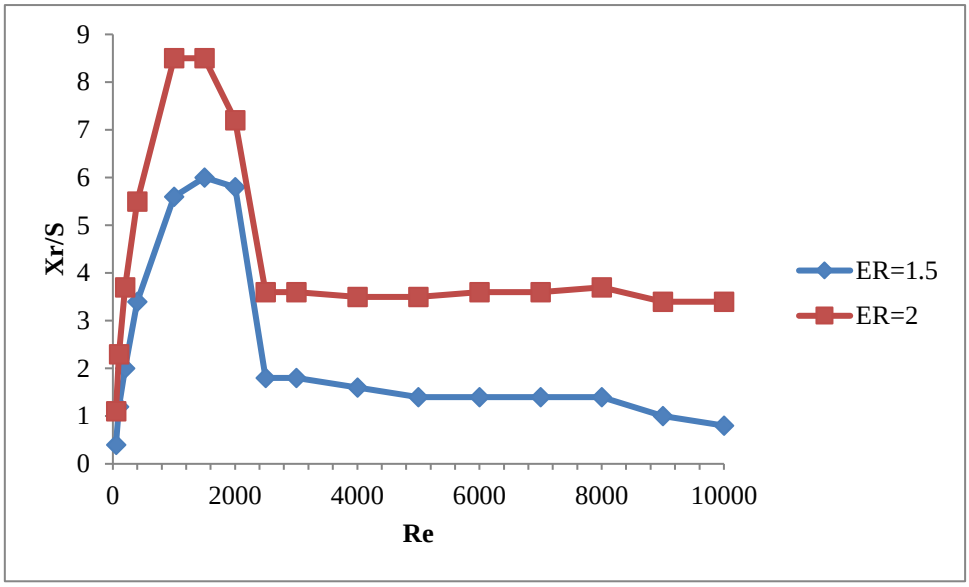

Figure 4.23: Effect of expansion ratio on Xr/S for different Re, R=0.005m.

4.3.4 Comparison of two dimensional vertical and curved backward facing step

Figure 4.24 shows the profile of the Nusselt number with the distance from the step normalised by the step height for vertical and curved step. The comparison is done at Reynolds number 100 and expansion ratio 2. From the Fig. 4.24 it is found that the peak for Nusselt number is higher for curved step and also shifted to the left side. The maximum value of Nusselt number is found near the reattachment point and as reattachment length is less for curved step the peak of Nusselt number shifts left for the curved step as compared to the vertical step.

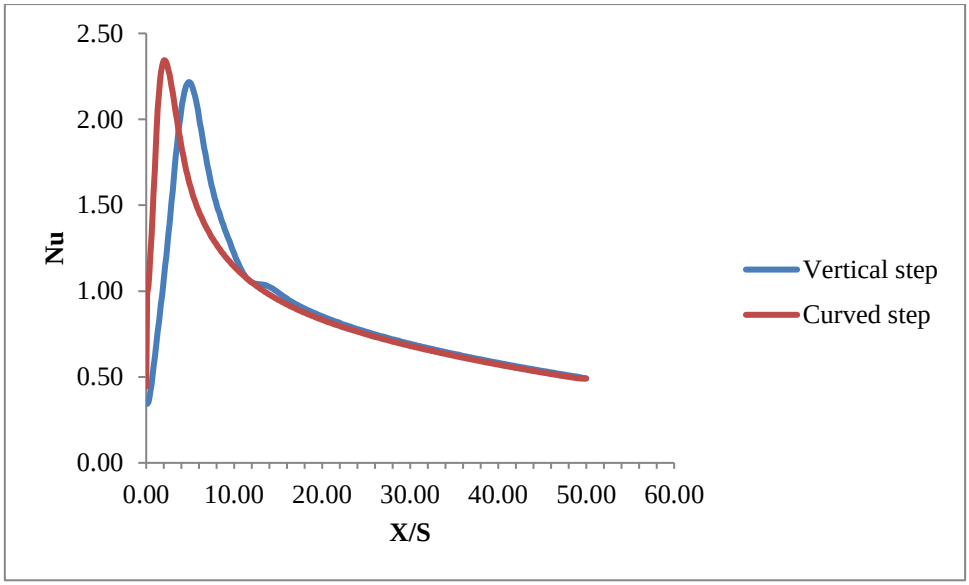

Figure 4.24: Comparison of Nu profile for 2-D vertical and curved step; Re=100, R=0.007m, ER=2.

Figure 4.25 shows the variation of Nusselt number with the Reynolds number covering laminar as well as turbulent flow. The comparison is made between the vertical step and the curved step having radius of curvature 0.007m. The magnitude of Nusselt number is found coinciding in the laminar and transition region up to Reynolds number 2500 for vertical and curved backward facing step. The Nusselt number is found increasing for the vertical step in the turbulent region for Reynolds number 2500 onwards.

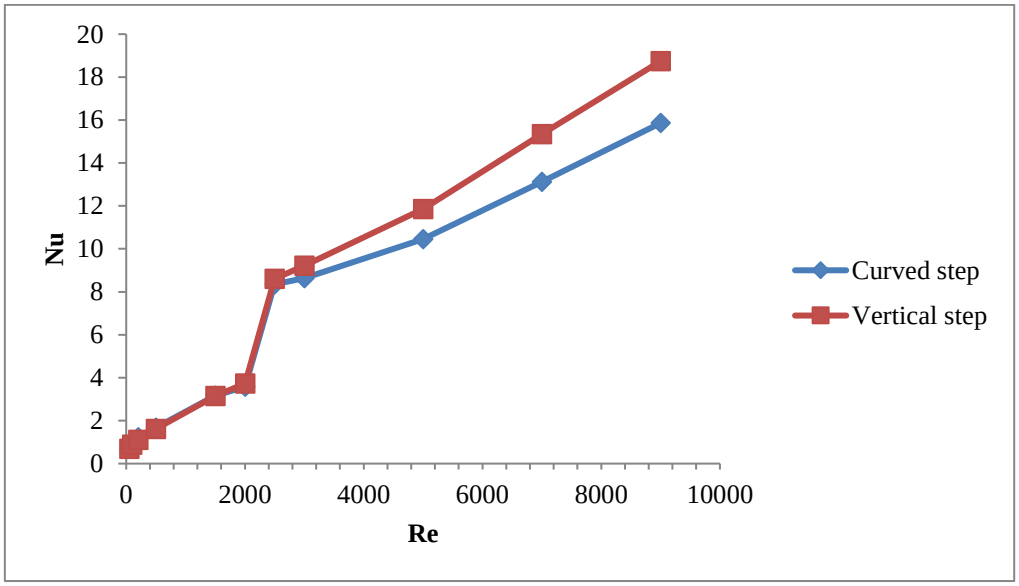

Figure 4.25: Comparison of Nu for curved and vertical step, ER=1.5, R=0.007m.

Figure 4.26 shows the variation of the reattachment length with the Reynolds number covering laminar as well as turbulent flow. The comparison is made between the vertical step and the curved step having radius of curvature 0.007m. The results are obtained for the expansion ratio 1.5. The reattachment length is found to increase in the laminar region and then decreases in the transition region and thereafter remains almost steady in the turbulent region for all expansion ratios. The magnitude of the reattachment length is found to be more for vertical backward facing step as compared to the curved backward facing step for all laminar, transition and turbulent regimes.

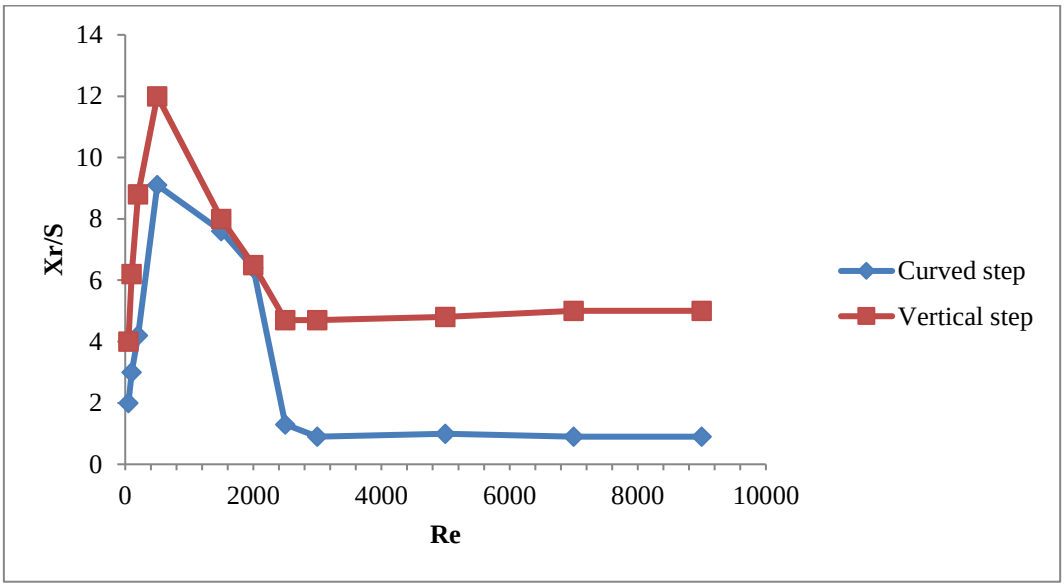

Figure 4.26: Comparison of reattachment length for curved and vertical step, ER=1.5, R=0.007m.

4.4 Three dimensional vertical backward facing step

The effect of Reynolds number and expansion ratio is studied on the Nusselt number and reattachment length. The study is performed for both laminar and turbulent flow. The results obtained are found to be in good agreement with Nie and Armaly, [2003].

4.4.1 Model validation

Nie and Armaly, [2003] developed a numerical model for the flow over a three dimensional backward facing step and studied the flow behaviour along with heat transfer characteristics in the recirculation zone. The present study considers the same geometry of backward facing step considered by Nie and Armaly, [2003] for the purpose of model validation. The

upstream height of the channel considered is 0.01m and the downstream height of the channel is 0.02m. The expansion ratio and aspect ratio considered are 2 and 8 respectively. The inlet temperature of the fluid is 20^0 C. The bottom downstream wall is heated at constant heat flux of 50 W/m^2.

4.4.2 Meshing quality parameters

The various mesh quality parameters are checked for the mesh generated in the geometry to ensure its quality. Table 4.2 shows the values of various mesh quality parameters for the 3-D vertical backward facing step and it is found that all the values of mesh parameters are lying within the permissible limits.

Table 4.2: Meshing quality parameters

Parameter	Value	Limiting Value
Maximum Skewness	0.84	< 0.95
Maximum Aspect Ratio	10.38	< 35
Orthogonal Quality	0.99	Close to 1

4.4.3 Grid independency test

The grid independency test is performed to make the results independent of the grid size after a particular number of elements. The present study considers three different cases for the grid independency test. The 3-D vertical backward facing step with expansion ratio 2 is discretized into 238375 elements for case 1 and then it is made finer by discretizing into 322988 and 436619 elements for case 2 and case 3 respectively. The model is simulated using governing equation represented in Eq. (3.5) to (3.11) along with the boundary conditions represented in section 3.3.6. The properties of air, convergence criteria and under relaxation factors represented in Table (3.3), (3.12) and (3.13) respectively are also used for the numerical simulation for all the three different cases. The nusselt number is determined for all the three different cases for Reynolds number 400. Table 4.3 shows the value of average Nusselt number on the heated downstream wall. It is found from the Table 4.3 that there is a significant change in the average value of nusselt number when the number of elements are increased from 238375 to 322988 but the change in results are insignificant for further increasing the number of elements in domain from 322988 to 436619. So the

optimum number of element is found to be 322988 which is used further for numerical simulation.

Table 4.3: Grid independency test for 3D vertical step [Nie and Armaly, 2003]

No. of elements	Nu_{avg}
238375	2.05
322988	2.12
436619	2.10

The numerical model developed in the present study is validated with the results given by Nie and Armaly, [2003]. Figure 4.27 shows the variation of Nusselt number with the distance from the step normalised by the step height which is found in good agreement with Nie and Armaly, [2003]. The all other results are obtained for the geometry taken according to Kondoh et al. [1993] where original study is performed for 2D backward facing step and in the current study the three dimensional investigation is carried out by extruding the two dimensional step in the positive z direction.

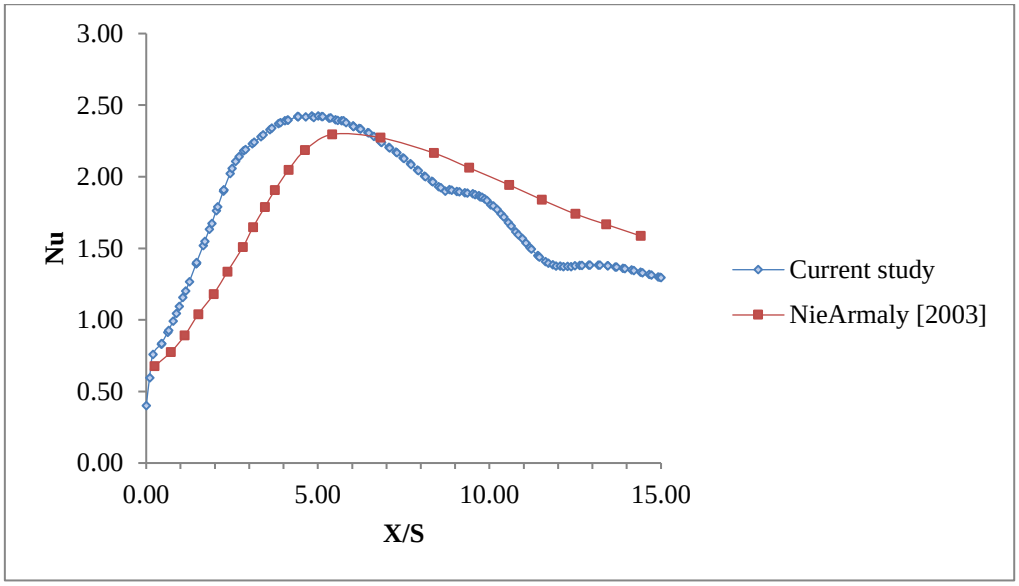

Figure 4.27: Comparison of Nusselt number for Re=400, Z/L=0.18, Y/S=0.01 ER=2.

4.4.4 Effect of Reynolds number

Figure 4.28 shows the effect of Reynolds number studied on the heat transfer characteristics through Nusselt number covering both the laminar and turbulent flow. The average value of Nusselt number is found to be increased with Reynolds number incessantly for both laminar

as well as turbulent flow. It is found clearly from the graph that there is sudden increase in the value of Nusselt number at Reynolds n umber 2500 due to turbulent characteristics of the flow.

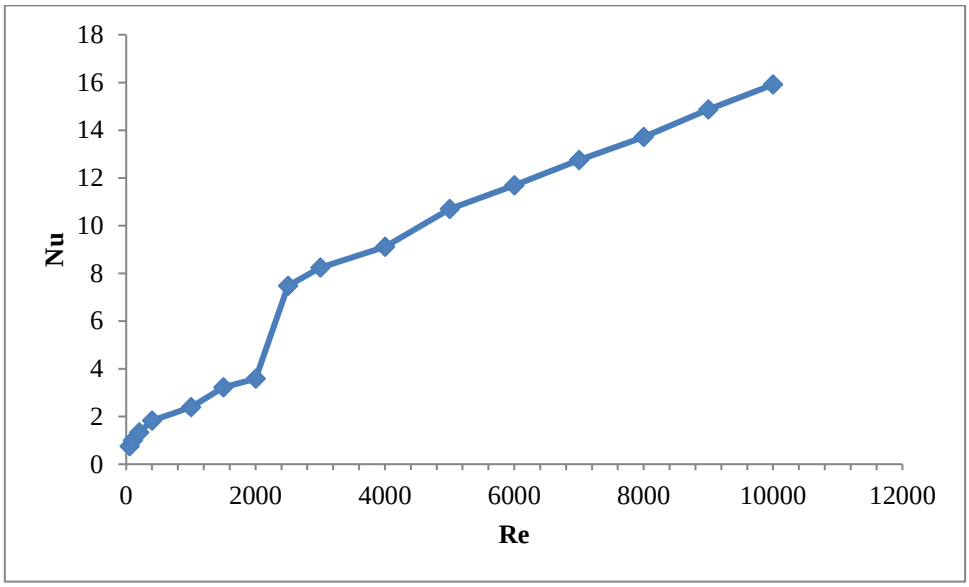

Figure 4.28: Variation of Nu with Re for 3-D vertical step, ER=1.5.

Figure 4.29 shows the variation of reattachment length with different Reynolds number covering laminar as well as turbulent flow with expansion ratio of 1.5. The reattachment length is found to be increased in the laminar region up to Reynolds number 1000. After that the reattachment length decreases in the transition region and remains lower throughout the turbulent range exhibiting almost static pattern.

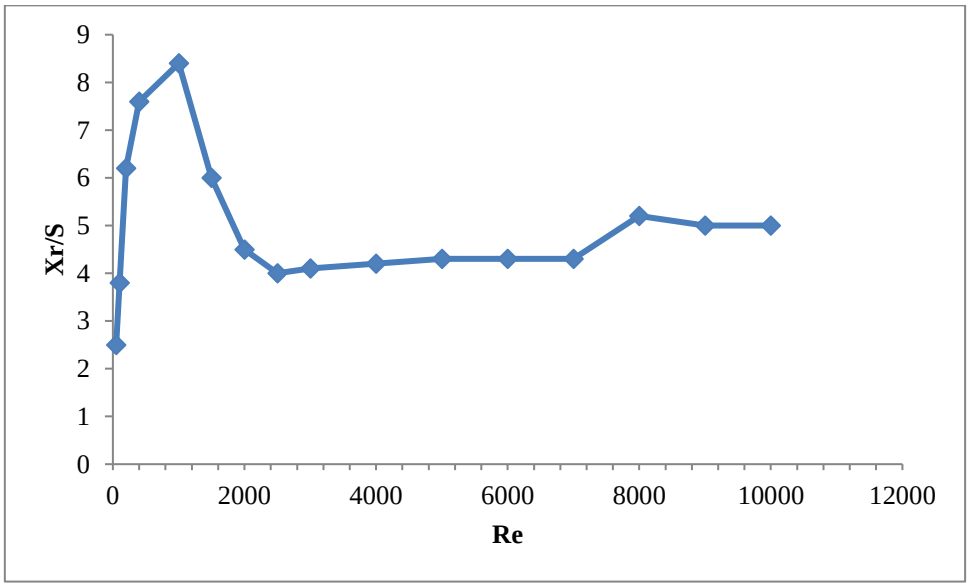

Figure 4.29: Variation of reattachment length with Re for 3-D vertical step, ER=1.5.

4.4.5 Effect of expansion ratio

The expansion ratio of a backward facing step can be changed by two ways, one is by varying the inlet channel height namely case 1 and another is by varying the step height namely case 2. Figure (4.30) to (4.31) belongs to case 1 and Fig. (4.32) to (4.33) belongs to case 2. Figure 4.30 shows the effect of expansion ratio on the Nusselt number for different Reynolds number covering laminar as well as turbulent flow. It is concluded from the graph that Nusselt number increases with increase in Reynolds number for different expansion ratio. The magnitude of Nusselt number is coinciding for different expansion ratio up to transition zone and there after the magnitude of Nusselt number lies below for the higher expansion ratio.

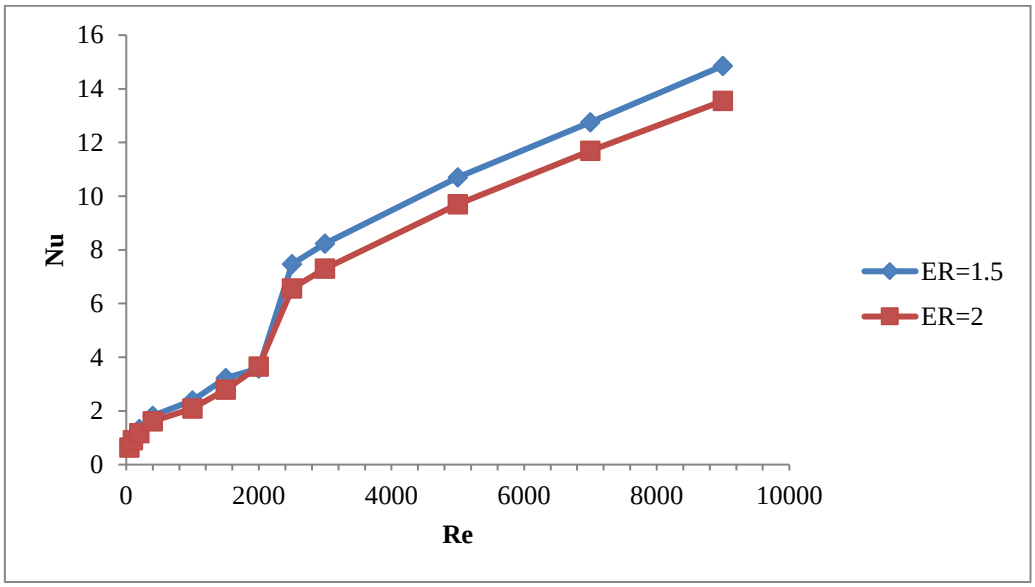

Figure 4.30: Variation of Nu with Re at different expansion ratios for 3-D vertical step.

Figure 4.31 shows the variation of the reattachment length with different Reynolds number covering laminar as well as turbulent flow for different expansion ratios 1.5 and 2. The reattachment length is found increasing with Reynolds number in the laminar region and then decreases in the transition region and thereafter remains almost steady in the turbulent region for all expansion ratios. The magnitude of the reattachment length for higher expansion ratio is found to be less during the laminar and transition flow and the magnitude of the reattachment length is found to be more in the turbulent regime for higher expansion ratio.

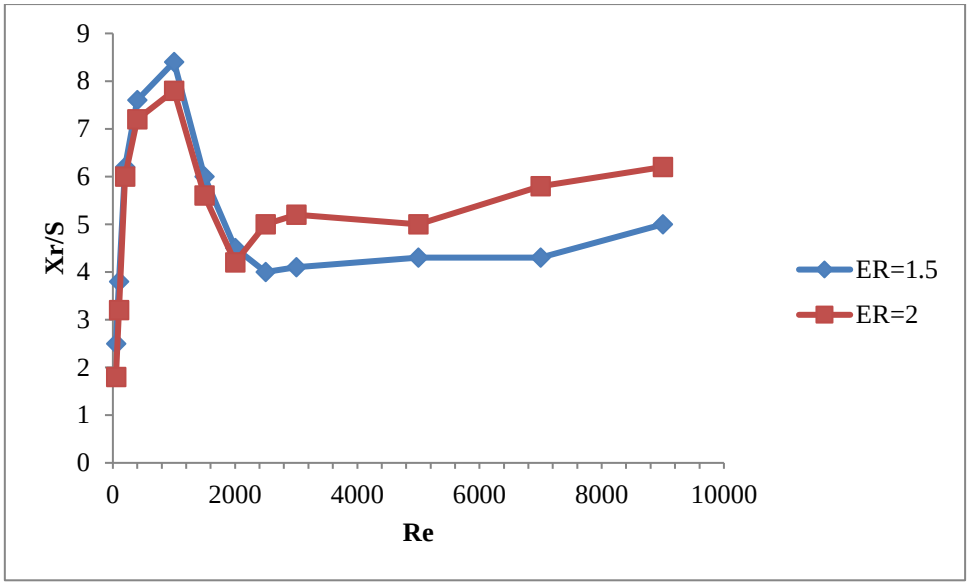

Figure 4.31: Variation of Xr/S with Re at different expansion ratios for 3-D vertical step.

Figure 4.32 shows the effect of expansion ratio on the Nusselt number for different Reynolds number covering laminar as well as turbulent flow. It is concluded from the graph that Nusselt number increases with increase in Reynolds number for different expansion ratio. The magnitude of Nusselt number is coinciding for different expansion ratio during the laminar and turbulent flow but found slightly lesser for higher expansion ratio in the transition regime.

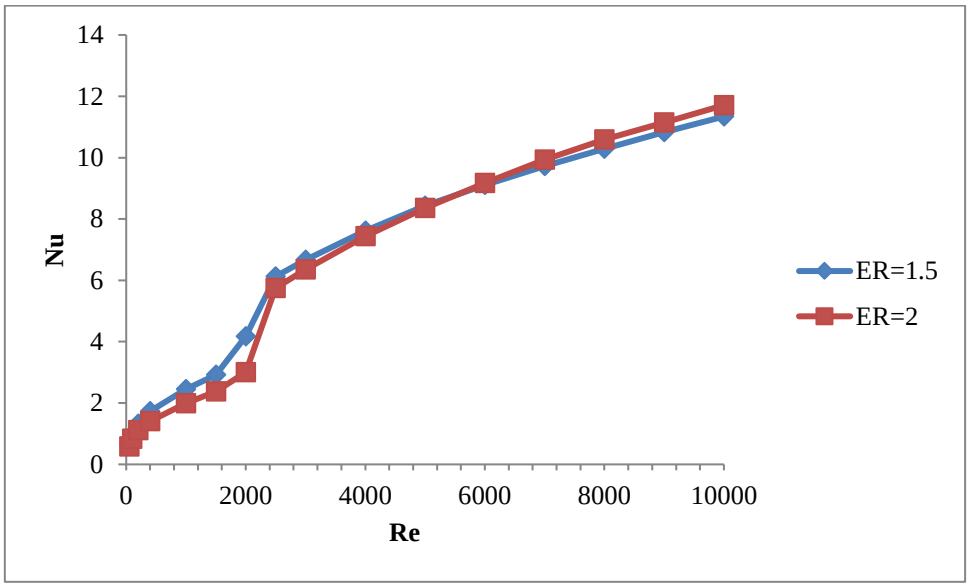

Figure 4.32: Variation of Nu with Re at different expansion ratios for 3-D vertical step.

Figure 4.33 shows the variation of the reattachment length with different Reynolds number covering laminar as well as turbulent flow for different expansion ratios 1.5 and 2. The reattachment length is found increasing with Reynolds number in the laminar region and then decreases in the transition region and thereafter remains almost steady in the turbulent region for all expansion ratios. The magnitude of the reattachment length for higher expansion ratio is found to be more for all laminar, transition and turbulent flow.

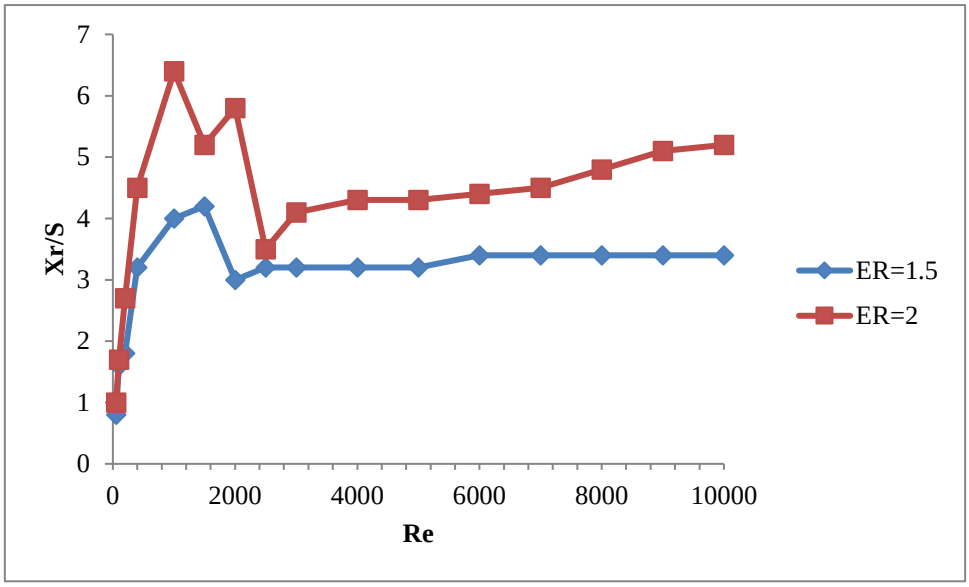

Figure 4.33: Variation of Xr/S with Re at different expansion ratios for 3-D vertical step.

4.4.6 Temperature profile

The temperature at any section downstream of backward facing step varies due to the heating of the bottom wall. So the thermal boundary layer develops due to change in temperature at a vertical section. The reason behind this profile is heating of bottom wall at constant temperature and top wall is set as adiabatic. Figure 4.34 shows the temperature profile drawn at the outlet along the vertical direction of the channel. The profile is obtained at the central plane for different Reynolds number ranging from 50-200 which is a laminar flow. It is found from Fig. 4.28 that the temperature of the fluid decreases in a parabolic fashion as we move from the bottom wall to the top wall. It is also found that the thermal boundary layer thickness decreases as the Reynolds number increases.

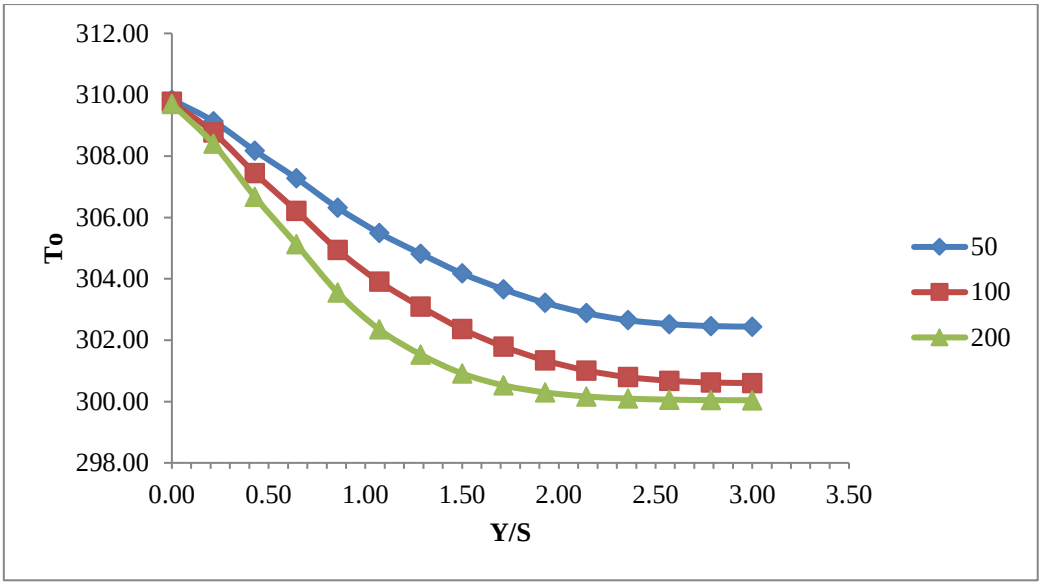

Figure 4.34: Temperature profile at outlet, Re=50,100,200; X=0.5m; Z=0.04m.

Similarly the temperature profile is determined for Reynolds number 3000, 5000 and 7000 which is lying in turbulent zone. Figure 4.35 shows the temperature profile drawn at outlet for turbulent flow. The Figure 4.35 shows that the temperature decreases in the vertical direction up to almost half the channel downstream width and after that it remains constant for turbulent flow. It is found that the gradient of thermal boundary layer for turbulent flow is steep in comparison to laminar flow. Also the thermal boundary layer thickness for turbulent flow is less in comparison to laminar flow due to continuous mixing of fluid layers.

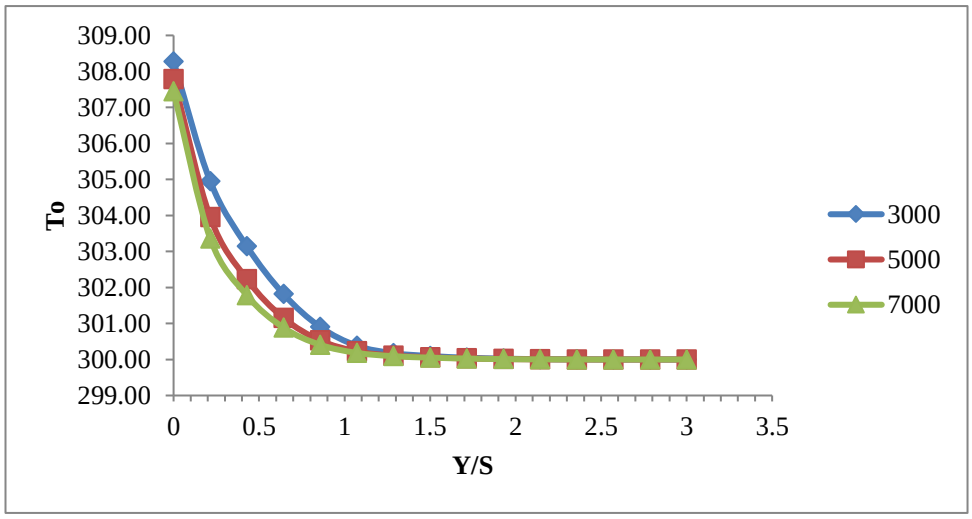

Figure 4.35: Temperature profile at outlet for turbulent flow; X=0.5m; Z=0.04m.

4.5 Three dimensional curved backward facing step

An attempt has been made to analyse the flow and heat transfer over the three dimensional curved backward facing step. The geometry along with dimensions of curved backward facing step considered in the present study are similar to Kondoh et al. [1993]. The radius of curved backward facing step is taken as 0.005m. The reattachment length and Nusselt number is calculated for various Reynolds number and compared with vertical backward facing step.

4.5.1 Effect on Nusselt number

Figure 4.36 shows the variation of average Nusselt number for 3-D curved backward facing step covering laminar as well as turbulent flow. The average Nusselt number has been calculated on the downstream heated wall. The average Nusselt number is observed to increase with Reynolds number for both laminar case and the turbulent case. There can be seen a sudden increase in the Nusselt number for Reynolds number 2500 due to turbulent nature of the flow.

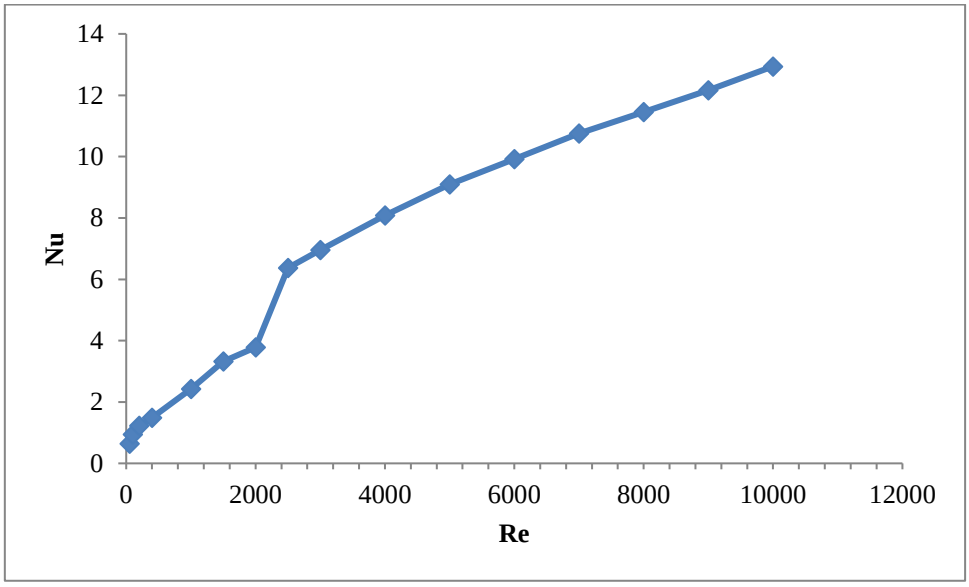

Figure 4.36: Variation of Nu vs Re for 3-D curved step, ER=2, R=0.005m, Y/S=0, Z/L=1

4.5.2 Effect on reattachment length

Figure 4.37 shows the variation of reattachment length different Reynolds number covering laminar as well as turbulent flow. The reattachment length is calculated at the central plane for the expansion ratio of 2 and radius of curvature 0.005m. The reattachment length is

observed to increase for the laminar flow up to Reynolds number 1000 and the reattachment length is found decreasing in the transition region from Reynolds number 1000-2500. The reattachment length has been found to remain almost static during the turbulent flow for Reynolds number 2500 onwards.

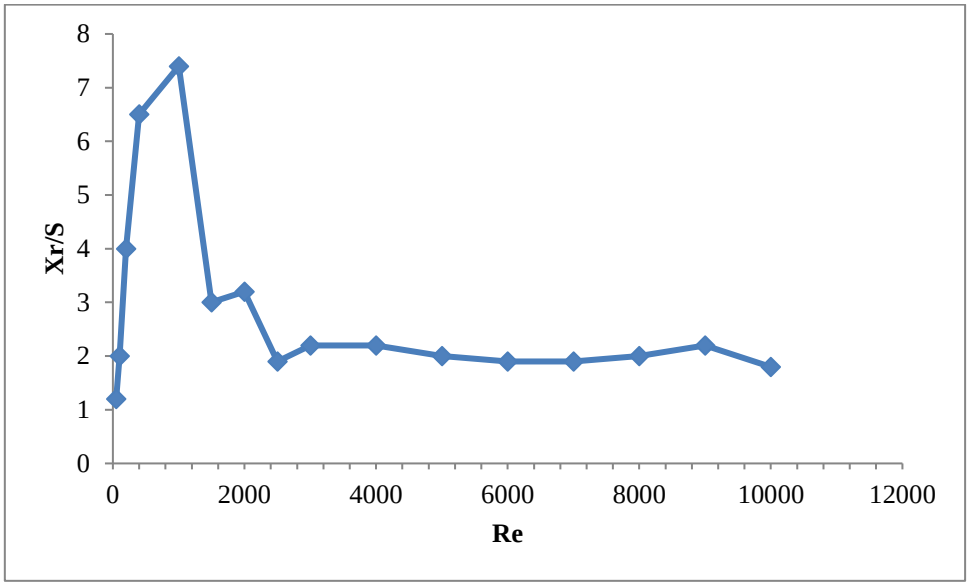

Figure 4.37: Variation of reattachment length with Re for 3-D curved step, ER=2, R=0.005, Z/L=1.

4.5.3 Effect of expansion ratio

The expansion ratio of a backward facing step can be changed by two ways, one is by varying the inlet channel height namely case 1 and another is by varying the step height namely case 2. Figure (4.38) to (4.39) belongs to case 1 and Fig. (4.40) to (4.41) belongs to case 2. Figure 4.38 shows the effect of expansion ratio on the Nusselt number for different Reynolds number covering laminar as well as turbulent flow. It is concluded from the graph that Nusselt number increases with increase in Reynolds number for different expansion ratio. The magnitude of Nusselt number is coinciding for different expansion ratio up to transition zone and there after the magnitude of Nusselt number lies below for the higher expansion ratio.

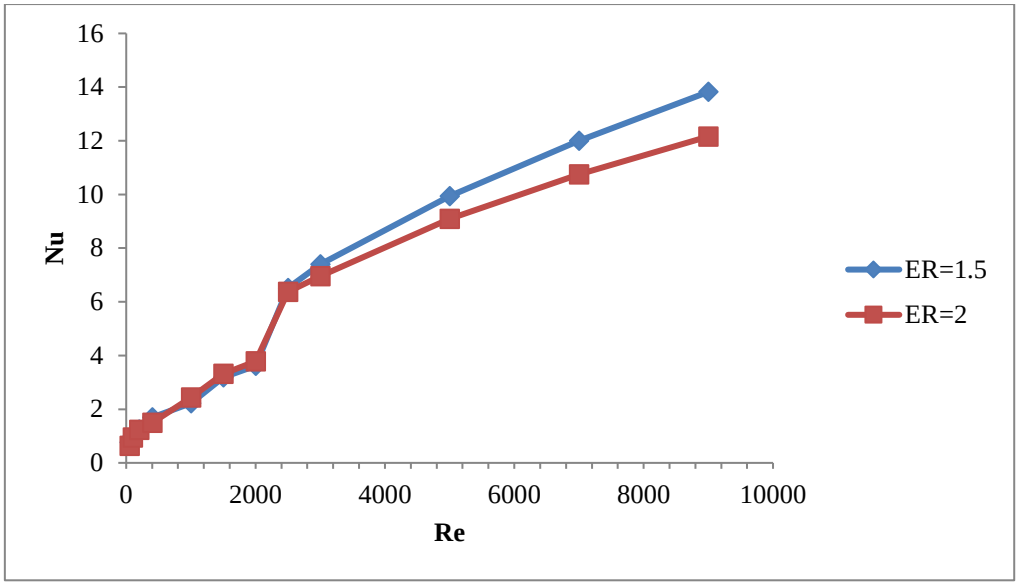

Figure 4.38: Effect of expansion ratio on Nu for different Re, R=0.005m.

Figure 4.39 shows the variation of the reattachment length with different Reynolds number covering laminar as well as turbulent flow for different expansion ratios 1.5 and 2. The reattachment length is found increasing with Reynolds number in the laminar region and then decreases in the transition region and thereafter remains almost steady in the turbulent region for all expansion ratios. The magnitude of the reattachment length for higher expansion ratio is found to be less during the laminar and transition flow and the magnitude of the reattachment length is found to be more in the turbulent regime for higher expansion ratio.

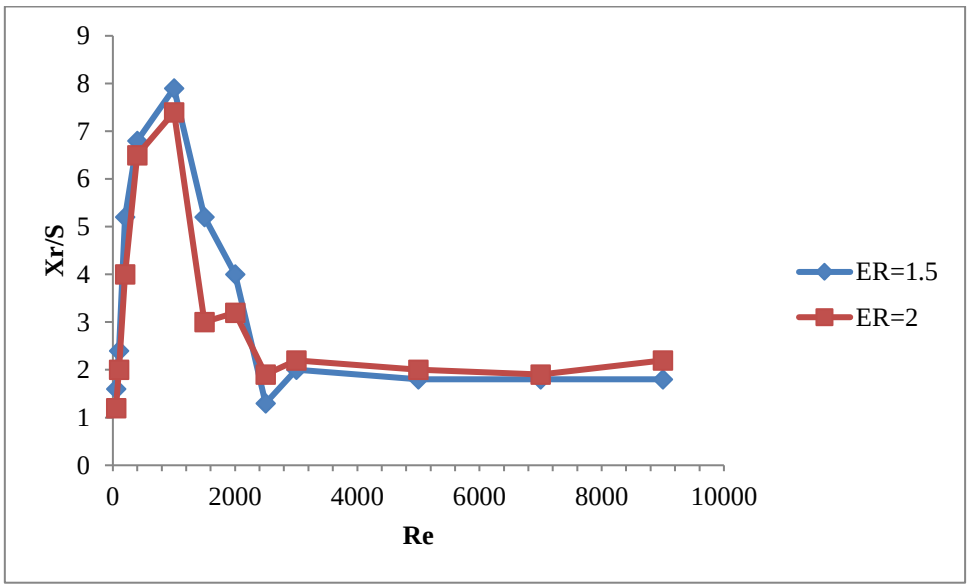

Figure 4.39: Effect of expansion ratio on Xr/S for different Re, R=0.005m.

Figure 4.40 shows the effect of expansion ratio on the Nusselt number for different Reynolds number covering laminar as well as turbulent flow. It is concluded from the graph that Nusselt number increases with increase in Reynolds number for different expansion ratio. The magnitude of Nusselt number is coinciding for different expansion ratio up to transition zone and there after the magnitude of Nusselt number lies below for the higher expansion ratio.

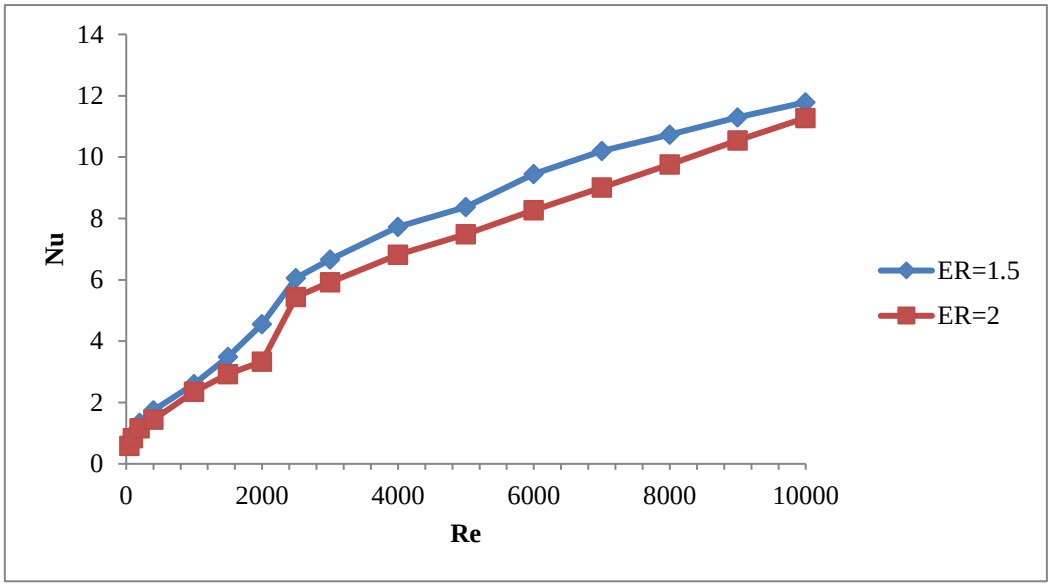

Figure 4.40: Effect of expansion ratio on Nu for different Re, R=0.005m

Figure 4.41 shows the variation of the reattachment length with different Reynolds number covering laminar as well as turbulent flow for different expansion ratios 1.5 and 2. The reattachment length is found increasing with Reynolds number in the laminar region and then decreases in the transition region and thereafter remains almost steady in the turbulent region for expansion ratio 1.5 but the reattachment length is found to be more fluctuating for higher expansion ratio 2. The magnitude of the reattachment length for higher expansion ratio is found to be more for all laminar, transition and turbulent flow regimes.

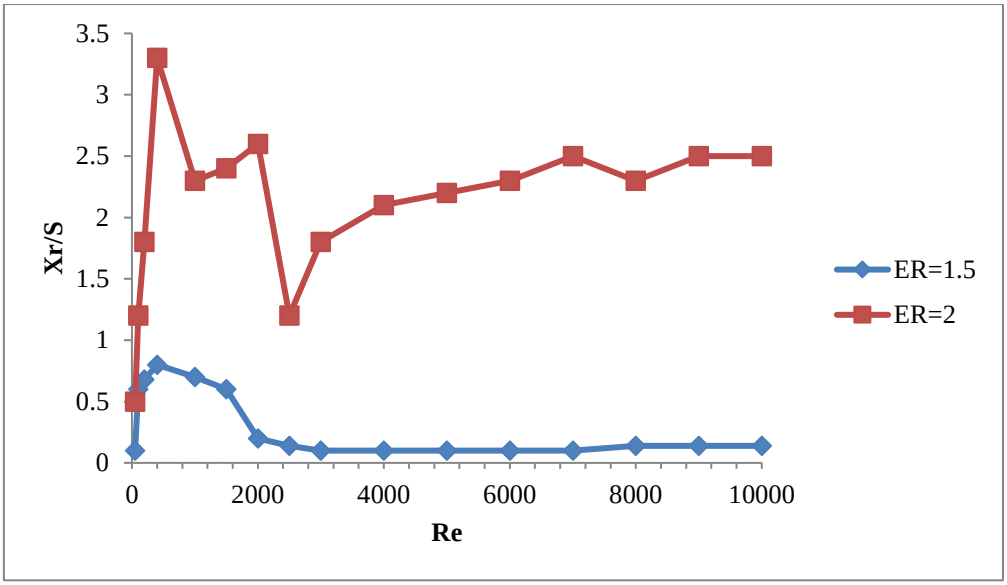

Figure 4.41: Effect of expansion ratio on Xr/S for different Re, R=0.005m.

4.6 Comparison of three dimensional vertical and curved backward facing step

The comparison has been made for the vertical and curved backward facing step. The average Nusselt number and the reattachment length are plotted with the Reynolds number covering laminar as well as turbulent flow.

4.6.1 Effect on Nusselt number

Figure 4.42 shows the variation of Nusselt number with the Reynolds number covering laminar as well as turbulent flow. The comparison is made between the vertical step and the curved step having radius of curvature 0.005m. The value of Nusselt number is found increasing with Reynolds number for vertical as well as curved step. The magnitude of Nusselt number is found coinciding in the laminar and transition region up to Reynolds number 2500 for vertical and curved backward facing step. The magnitude of Nusselt number is found increasing for the vertical backward facing step as compared to the curved backward facing step in the turbulent region for Reynolds number 2500 onwards.

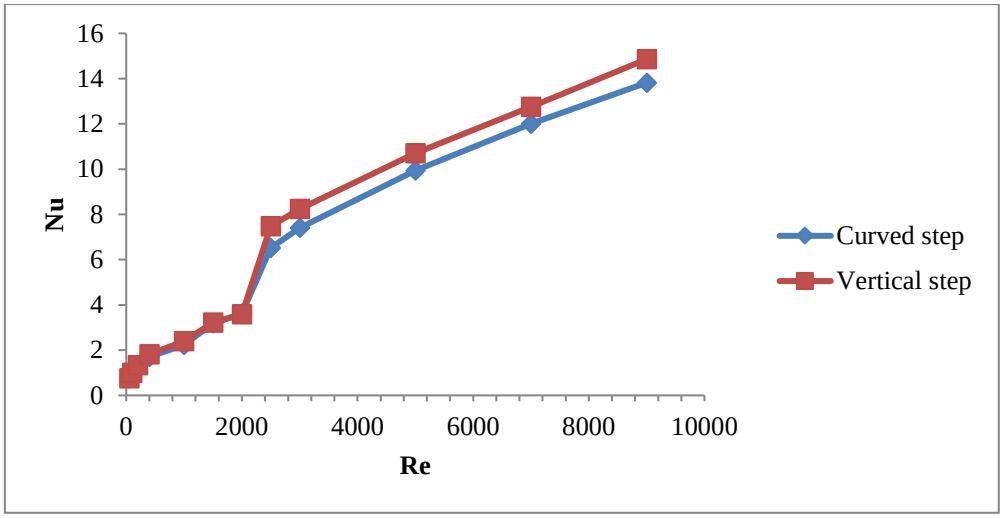

Figure 4.42: Comparison of Nu for 3-D curved and vertical step, ER=1.5, R=0.005m.

4.6.2 Effect on reattachment length

Figure 4.43 shows the variation of the reattachment length with the Reynolds number covering laminar as well as turbulent flow. The comparison is made between the vertical step and the curved step having radius of curvature 0.005m. The results are obtained for the expansion ratio 1.5. The reattachment length is found to increase in the laminar region and then decreases in the transition region and thereafter remains almost steady in the turbulent region for all expansion ratios. The magnitude of the reattachment length is found to be more for vertical backward facing step as compared to the curved backward facing step for all laminar, transition and turbulent regimes.

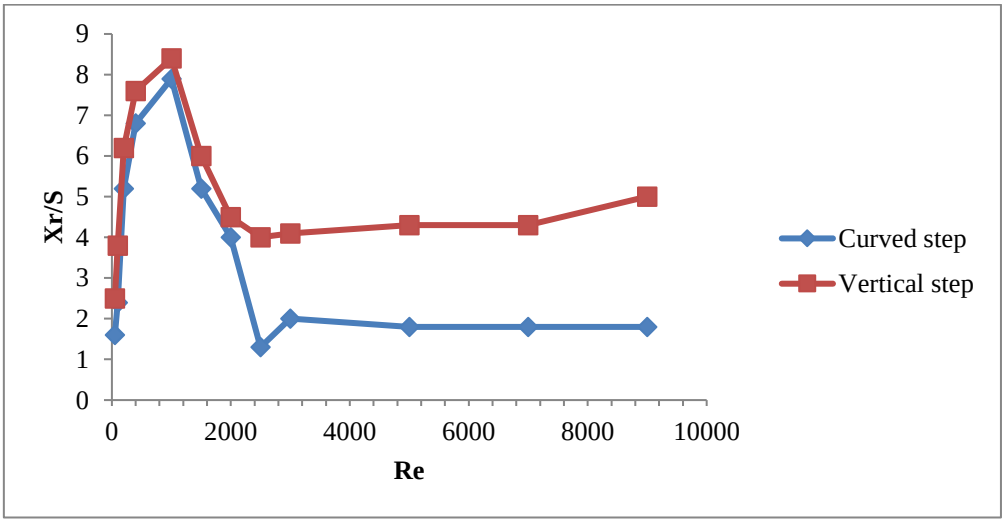

Figure 4.43: Comparison of reattachment length for 3-D curved and vertical step, ER=1.5, R=0.005m

4.7 Concluding remarks

The results of the present study has been analysed for both vertical backward facing step and the curved backward facing step. The results for the reattachment length and Nusselt number are calculated for wide range of Reynolds number covering laminar as well as turbulent flow. The reattachment length has been found to increase in the laminar region and starts decreasing in the transition region at Reynolds number 1500 onwards. A steep decline in the reattachment length is found to occur in the turbulent region at Reynolds number 2500 onwards. The reattachment length is observed to remain almost steady during the turbulent flow regime.

The results calculated for the reattachment length are observed for both vertical backward facing step and curved backward facing step. The reattachment length is observed to decrease with increase in the expansion ratio for laminar flow whereas reattachment length is found increasing with increase in the expansion ratio for turbulent flow. The reattachment length is also found to be less for curved backward facing step as compared to the vertical backward facing step.

The results for the Nusselt number are also calculated for wide range of Reynolds number incorporating both the laminar and turbulent flow. The value of Nusselt number is observed to increase with the Reynolds number both in laminar and turbulent case. The steep increase in the Nusselt number is found as we stepped into the turbulent flow at Reynolds number 2500. The results for Nusselt number are also compared for vertical backward facing step and curved backward facing step. The peak of the Nusselt number is observed to be shifted towards left for the curved backward facing step as compared to the vertical backward facing step due to decrease in the reattachment length for the curved backward facing step.

Chapter 5

Conclusions and Future Scope

5.1 Conclusions

Flow over a backward facing step along with heat transfer is studied for two and three dimensional vertical as well as curved backward facing step using ANSYS Fluent. The reattachment length and Nusselt number are calculated for a wide range of Reynolds number covering both laminar and turbulent flow. Also the reattachment length and Nusselt number are calculated for various expansion ratios. The results are validated with published literature. The flow characteristics are obtained for vertical backward facing step as well as for the curved backward facing step incorporating laminar as well as turbulent flow. The results obtained from the curved backward facing step are compared with the vertical backward facing step.

The results for the reattachment length and Nusselt number are calculated for wide range of Reynolds number covering laminar as well as turbulent flow. The reattachment length has been found to increase in the laminar region and starts decreasing in the transition region at Reynolds number 1500 onwards. A steep decline in the reattachment length is found to occur in the turbulent region at Reynolds number 2500 onwards. The reattachment length is observed to remain almost steady during the turbulent flow regime. The results calculated for the reattachment length are observed for both vertical backward facing step and curved backward facing step. The reattachment length is observed to decrease with increase in the expansion ratio for laminar flow whereas reattachment length is found increasing with increase in the expansion ratio for turbulent flow when the expansion ratio is varied by changing the inlet channel height. The reattachment length is found to increase with increase in expansion ratio for all laminar, transition and turbulent flow regimes when expansion ratio is varied by changing the step height. The reattachment length is also found to be less for curved backward facing step as compared to the vertical backward facing step.

The results for the Nusselt number are also calculated for wide range of Reynolds number incorporating both the laminar and turbulent flow. The value of Nusselt number is observed to increase with the Reynolds number both in laminar and turbulent case. The steep increase in the Nusselt number is found as we stepped into the turbulent flow at Reynolds

number 2500. The results for Nusselt number are also compared for vertical backward facing step and curved backward facing step. The peak of the Nusselt number is observed to be shifted towards left for the curved backward facing step as compared to the vertical backward facing step due to decrease in the reattachment length for the curved backward facing step.

5.2 Future scope

The present study has been conducted to study the effect of Reynolds number and expansion ratio on the heat transfer and reattachment length for vertical as well as curved backward facing step.

1. In future the analysis of reattachment length and heat transfer can be done for inclined backward facing step providing different angles of inclination.

2. The investigation can also be carried out to study the two kind of instability prevailing during the flow over a backward facing step namely Kelvin-Helmholtz instability and Taylor-Gortler like instability for vertical, curved and inclined backward facing step.

3. The variation of Nusselt number can be studied in the span wise direction of the backward facing step.

References

Abu-Mulaweh H.I., Armaly B.F., Chen T.S. (1993) Measurements of laminar mixed convection in boundary-layer flow over horizontal and inclined backward-facing steps. *International journal of heat and mass transfer*, 36: 1883-1895.

Al-aswadi A.A., Mohammed H.A., Shuaib N.H., Campo A. (2010) Laminar forced convection flow over a backward facing step using nanofluids. *International communications in heat and mass transfer*, 37: 950-957.

Armaly B.F., Durst F., Pereira J.C.F., Schonung B. (1983) Experimental and theoretical investigation of backward facing step flow. *Journal of fluid mechanics*, 127: 473-496.

Aung W. (1983) An experimental study of laminar heat transfer downstream of backsteps. *Journal of heat transfer*, 105: 823-829.

Barkley D., Gomes M.G.M., Henderson R.D. (2002) Three dimensional instability in flow over backward facing step. *Journal of fluid mechanics*, 473: 167-190.

Biswas G., Breuer M., Durst F. (2004) Backward facing step flows for various expansion ratios at low and moderate Reynolds numbers. *Journals of fluid engineering*, 126: 362-374.

Chen C., Yen T., Yang Y. (2005) Lattice Boltzmann method simulation of backward facing step on convective heat transfer with field synergy principle. *International journal of heat and mass transfer*, 49: 1195-1204.

Chen Y.T., Nie J.H., Armaly B.F., Hsieh H.T. (2006) Turbulent separated convection flow adjacent to backward facing step-effects of step height. *International journal of heat and mass transfer*, 49: 3670-3680.

Dejoan A., Leschziner M. (2004) Large eddy simulation of periodically perturbed separated flow over a backward facing step. *International journal of heat and fluid flow*, 25: 581-592.

Driver D.M., Seegmiller H.L., Marvin J.G. (1987) Time dependent behaviour of a reattaching shear layer. *AIAA journal*, 25: 914-919.

Erturk E. (2008) Numerical solutions of 2D steady incompressible flow over a backward facing step. *Journals of computers and fluids*, 37: 633-655.

Gautier N., Aider J.L. (2014) Upstream open loop control of the recirculation area downstream of a backward facing step. *Comptes rendus mecanique*, 342: 382-388.

Hattori H., Nagano Y. (2012) Structures and mechanism of heat transfer phenomena in turbulent boundary layer with separation and reattachment via DNS. *International journal of heat and fluid flow*, 37: 81-92.

Iwai H., Nakabe K., Suzuki K. (2000) Flow and heat transfer characteristics of backward facing step laminar flow in a rectangular duct. *International journal of heat and mass transfer*, 43: 457-471.

Kanna P.R., Das M.K. (2007) Conjugate heat transfer study of a two dimensional laminar incompressible wall jet over a backward facing step. *Journal of heat transfer*, 129: 220-231.

Kapiris P.G., Mathioulakis D.S. (2014) Experimental study of vortical structures in a periodically perturbed flow over a backward facing step. *International journal of heat and fluid flow*, 47: 101-112.

Khanafer K., Al-Azmi B., Al-Shammari A., Pop I. (2005) Mixed convection analysis of laminar pulsating flow and heat transfer over a backward-facing step. *International journal of heat and mass transfer*, 51: 5785-5793.

Kherbeet A.S., Mohammed H.A., Salman B.H. (2012) The effect of nanofluids flow on mixed convection heat transfer over microscale backward facing step. *International journal of heat and mass transfer*, 55: 5870-5881.

Kondoh T., Nagano Y., Tsuji T. (1993) Computational study of laminar heat transfer downstream of a backward facing step. *International journal of heat and mass transfer*, 36: 577-591.

Lan H., Armaly B.F., Drallmeier J.A. (2009) Three-dimensional simulation of turbulent forced convection in a duct with backward-facing step. *International journal of heat and mass transfer*, 52: 1690-1700.

Lancial N., Beaubert F., Harmand S., Rolland G. (2013) Effects of a turbulent wall jet on heat transfer over a non confined backward facing step. *International journal of heat and fluid flow*, 44: 336-347.

Le H., Moin P., Kim J. (1997) Direct numerical simulation of turbulent flow over a backward facing step. *Journal of fluid mechanics*, 330: 349-374.

Lee T., Mateescu D. (1998) Experimental and numerical investigation of 2D backward facing step flow. *Journals of fluid and structures*, 12: 703-716.

Lima R.C., Andrade C.R., Zaparoli E.L. (2008) Numerical study of three recirculation zones in the unilateral sudden expansion flow. *International communications in heat and mass transfer*, 35: 1053-1060.

Nie J.H., Armaly B.F. (2002) Three-dimensional convective flow adjacent to adjacent to backward facing step-effects of step height. *International journal of heat and mass transfer*, 45: 2431-2438.

Nie J.H., Armaly B.F. (2003) Reattachment of three dimensional flow adjacent to backward facing step. *Journal of heat transfer*, 125: 422-428.

Oztop H.F., Mushatet K.S., Yilmaz I. (2012) Analysis of turbulent flow and heat transfer over a double forward facing step with obstacles. *International communications in heat and mass transfer*, 39: 1395-1403.

Rani H.P., Sheu T.W.H., Tsai E.S.F. (2007) Eddy structures in a transitional backward facing step flow. *Journal of fluid mechanics*, 288: 43-58.

Ratha D., Sarkar A. (2014) Analysis of flow over backward facing step with transition. *Frontiers of Structural and Civil Engineering*, 9: 71-81.

Rouizi Y., Girault M., Favennec Y., Petit D. (2010) Model reduction by the modal identification method in forced convection. *International journal of thermal sciences*, 49: 1354-1368.

Saldana J.G., Anand N.K., Sarin V. (2005) Numerical simulation of mixed convective flow over a three-dimensional horizontal backward facing step. *Journal of heat transfer*, 127: 1027-1036.

Shih C., Ho C.M. (1994) Three dimensional recirculation flow in a backward facing step. *Journal of fluid engineering*, 116: 228-232.

Simpson R.L. (1996) Aspects of turbulent boundary layer separation. Prog. *Aerospace Sci.*, 32: 457-521.

Terhaar S., Velasquez A., Arias J. R., Sanchez-Sanz M. (2010) Experimental study on unsteady laminar heat transfer downstream of backward facing step. *Journal of heat and mass transfer*, 37: 457-462.

Tinney C.E., Ukeiley L.S. (2009) A study of 3-D backward facing step. *Exp fluids*, 47: 427-438.

Togun H., Abdulrazzaq T., Kazi S.N., Badarudin A., Ariffin M.K.A., Zubir M.N.M. (2014) Numerical study of heat transfer and laminar flow over a backward facing step with and without obstacle. *International journal of mechanical, aerospace, industrial and manufacturing engineering*, 8: 2.

Togun H., Abdulrazzaq T., Kazi S.N., Badarudin A., Ariffin M.K.A. (2013) Heat transfer to laminar flow over a double backward facing step. *International journal of mechanical, aerospace, industrial and manufacturing engineering*, 7: 8.

Velazquez A., Arias J.R., Mendez B. (2008) Laminar heat transfer enhancement downstream of a backward facings step by using a pulsating flow. *International journal of heat and mass transfer*, 51: 2075-2089.

Vogel J.C., Eaton J.K. (1985) Combined heat transfer and fluid measurements downstream of a backward facing step. *Journal of heat transfer*, 107: 922-929.

Wu Y., Christensen K.T. (2010) Spatial structures of a turbulent boundary layer with irregular surface roughness. *Journal of fluid mechanics*, 655: 380-418.

Wu Y., Ren H., Tang H. (2013) Turbulent flow over a rough backward facing step. *International journal of heat and fluid flow*, 44: 155-169.